TECHNICAL REPORT STANDARD TITLE PAGE

1. Report No.	2. Government Accession No.	3. Recipient's Catalog No.

4. Title and Subtitle	5. Report Date
"The Behavior of Multiple Lap Splices in Wide Sections"	January 1975
	6. Performing Organization Code

7. Author(s)	8. Performing Organization Report No.
Mark A. Thompson, James O. Jirsa, John E. Breen, and Donald F. Meinheit	Research Report 154-1

9. Performing Organization Name and Address	10. Work Unit No.
Center for Highway Research The University of Texas at Austin Austin, Texas 78712	11. Contract or Grant No. Research Study 3-5-72-154
	13. Type of Report and Period Covered Interim
12. Sponsoring Agency Name and Address Texas Highway Department Planning & Research Division P. O. Box 5051 Austin, Texas 78763	14. Sponsoring Agency Code

15. Supplementary Notes

Work done in cooperation with the Federal Highway Administration, Department of Transportation.
Research Study Title: "Factors Affecting Splice Development Length"

16. Abstract

In most reinforced concrete cantilever retaining walls, construction procedures require some type of splicing of the reinforcing steel. Economics often dictate the use of a lap splice. Since a retaining wall has no redundancy, understanding of splice behavior becomes critical to the design of the structure.

In order to investigate the behavior of lap splices of the reinforcing steel in such a structure, twenty-five specimens were tested. The specimens were tested with the splice regions subjected to a constant moment along the length of the splice. This loading produced a stress condition as severe as that in the prototype. The main variables in the test program were the splice length and bar diameter, the ratio of the clear cover to the clear spacing of the splices, the edge splice condition, the amount of transverse reinforcement in the splice region, and the casting position. Cracking patterns, steel strain distributions, and failure modes of the specimens were studied to obtain a basic understanding of the behavior of lap splices in wide sections.

17. Key Words	18. Distribution Statement
lap splices, behavior, retaining wall, test, failure	

19. Security Classif. (of this report)	20. Security Classif. (of this page)	21. No. of Pages	22. Price
Unclassified	Unclassified	89	

Form DOT F 1700.7 (8-69)

THE BEHAVIOR OF MULTIPLE LAP SPLICES IN WIDE SECTIONS

by

Mark A. Thompson
James O. Jirsa
John E. Breen
and
Donald F. Meinheit

Research Report No. 154-1

Research Project No. 3-5-72-154

Factors Affecting Splice Development Length

Conducted for

The Texas Highway Department

In Cooperation with the
U. S. Department of Transportation
Federal Highway Administration

by

CENTER FOR HIGHWAY RESEARCH
THE UNIVERSITY OF TEXAS AT AUSTIN

January 1975

The contents of this report reflect the views of the authors, who are responsible for the facts and the accuracy of the data presented herein. The contents do not necessarily reflect the official views or policies of the Federal Highway Administration. This report does not constitute a standard, specification, or regulation.

PREFACE

This report presents the results of a study of lapped splices in wide sections. Twenty-five wall-type specimens containing five or six splices were tested to determine the influence of splice length, bar diameter, ratio of clear cover to clear spacing, edge splice conditions, and transverse reinforcement on the splice strength. Comparisons of measured to predicted strength were made using current and proposed design recommendations.

This is the first report on work conducted under Project 3-5-72-154, "Factors Affecting Splice Development Length." Subsequent reports will describe experimental work on the behavior of splices under impact loading (154-2) and on reevaluation of splice and development length data aimed at producing new design recommendations (154-3F). The program was sponsored by the Texas Highway Department and the Federal Highway Administration and administered by the Center for Highway Research at The University of Texas at Austin. Close liaison with the Texas Highway Department has been maintained through Mr. Wesley Pair and with the Federal Highway Administration through Mr. Jerry Bowman.

The project was under the general direction of Professor J. E. Breen and the immediate supervision of Professor J. O. Jirsa. The authors gratefully acknowledge the staff of the Civil Engineering Structures Research Laboratory at the Balcones Research Center of The University of Texas at Austin for their assistance in carrying out the experimental studies.

A B S T R A C T

In most reinforced concrete cantilever retaining walls, construction procedures require some type of splicing of the reinforcing steel. Economics often dictate the use of a lap splice. Since a retaining wall has no redundancy, understanding of splice behavior becomes critical to the design of the structure.

In order to investigate the behavior of lap splices of the reinforcing steel in such a structure, twenty-five specimens were tested. The specimens were tested with the splice regions subjected to a constant moment along the length of the splice. This loading produced a stress condition as severe as that in the prototype. The main variables in the test program were the splice length and bar diameter, the ratio of the clear cover to the clear spacing of the splices, the edge splice condition, the amount of transverse reinforcement in the splice region, and the casting position. Cracking patterns, steel strain distributions, and failure modes of the specimens were studied to obtain a basic understanding of the behavior of lap splices in wide sections.

Failure modes of wall section splices were identified and classified according to the ratio of the edge cover to the clear cover for the specimens containing all bars spliced. Failure patterns of specimens having continuous edge bars or transverse reinforcement were also discussed. The various factors critical to splice strength were examined. In general, an increase in the lap length, ratio of the clear cover to the clear spacing, amount of transverse reinforcement in the splice region or concrete strength produced an increased strength of the splice. Top casting the main reinforcement was shown to be detrimental to splice strength.

It was concluded that increased edge cover or the use of continuous edge bars would not result in a substantial increase in the strength of a section containing a number of splices (e.g., a retaining wall). Therefore, it was recommended that for design considerations no distinction be made

between edge or interior splices. Prevailing ACI and AASHTO code provisions for splices predicted strengths which were very conservative when applied to the specimens tested. Because current provisions omit many parameters critical to splice strength and greatly underestimate the strength of such a section, splice data were reevaluated and an empirical equation for splice design was developed in an accompanying study. Excellent agreement was exhibited between the empirical equation and the results of the wall-type specimens.

KEY WORDS: lap splices, behavior, retaining wall, test, failure.

S U M M A R Y

Twenty-five specimens were tested to determine the behavior of lap splices of the reinforcement in a cantilever wide section. Failure patterns were observed and categorized according to the ratio of the edge cover to the clear bottom cover. The various factors shown to be influential to splice strength were presented and discussed.

Based on the test results obtained from this study, the following conclusions were made. The strength of the splice section in a wall-type specimen seemed to be governed by the capacity of the interior splices, such that a modification of edge conditions did not drastically affect total splice section strength. Prevailing ACI and AASHTO code specifications for length of splices were safe when applied to the wall splices tested. However, the current provisions greatly underestimate splice strength because many of the parameters critical to splice strength are not reflected in the equations.

I M P L E M E N T A T I O N

The results of the test program contained in this report describe the behavior of tension lap splices of the reinforcing steel in cantilever wide sections. The strength of a splice section in a wall is basically governed by the capacity of the interior splices. A modification of edge conditions in a wall splice section to obtain a higher splice strength does not appear to be warranted.

Splice behavior was greatly improved with the addition of transverse reinforcement in the splice region. For structures where ductile performance is required, a minimum amount of transverse reinforcement in the splice section should be considered.

Wall splices based on the current ACI and AASHTO specifications are quite conservative. Some modification of existing provisions appears to be feasible without compromising the safety of retaining wall structures.

TABLE OF CONTENTS

Chapter Page

L I S T O F T A B L E S

L I S T O F F I G U R E S

NOTATION

A_b	Cross-sectional area of longitudinal steel bar, $in.^2$
A_{tr}	Cross-sectional area of transverse reinforcement at a given spacing, s, per longitudinal bar, $in.^2$
b	Width of section, in.
c	Clear bottom cover over longitudinal bars, in.
C	Smaller of c, H, or $S'/2$, in.
d_b	Diameter of longitudinal reinforcement, in.
d	Effective depth of section, in.
f'_c	Compressive strength of concrete, psi.
f_s	Stress in longitudinal reinforcement, psi.
f'_t	Split tensile strength of concrete, psi
f_y	Yield strength of longitudinal reinforcement, psi.
f_{yt}	Yield strength of transverse reinforcement, psi.
H	Edge cover, in.
ℓ_s	Splice length, in.
n	Number of longitudinal bars in a section.
P	Total load applied to end of specimen, kips.
P_d	Equivalent dead load applied to one end of specimen, kips.
P_y	Total load applied to end of specimen required to yield main reinforcement, kips.
S'	Clear spacing between splices, in.
s	Effective spacing of transverse reinforcement, in.
t	Depth of section, in.
u	Average bond stress, psi.
ρ	nA_b/bd
ρ_v	A_{tr}/sb

CHAPTER 1

INTRODUCTION

1.1 Object and Scope

The object of this study was to examine the strength and behavior of wide sections containing multiple lap splices. Twenty-five specimens were constructed to simulate splice conditions in a typical cantilever retaining wall section with the main reinforcement in the wall stem lap spliced to anchor bars that extend up from the base. The test specimens contained either five or six #6, #8, #11, or #14 bars lap spliced in a section that varied from 33 to 45 in. in width. The basic variables in the test program were the splice length and bar diameter, the ratio of clear cover to the clear spacing of the splices, the edge splice condition, the amount of transverse reinforcement in the splice region, and the casting position. The concrete strength varied from 2525 to 4710 psi. The behavior of the wide sections containing spliced bars is discussed and evaluated with regard to each of the variables. An evaluation of current and proposed splice strength equations as applied to wall splices is presented.

1.2 Definition of the Problem

For a typical cantilever retaining wall, construction procedures normally require lap splicing of the reinforcing steel at the junction of the wall and the base. This junction is a region of peak moment in the wall, and a splice failure in such a situation would mean failure of the wall, since the structure has no redundancy. Therefore, an understanding of the behavior of lapped splices is essential to the design of a retaining wall.

The performance of lap splices in narrow beam sections has been the subject of extensive investigation. Tests indicated that the failure

of spliced sections may initiate at an edge. The behavior patterns of wall splices have been studied but not completely bounded, due to limitations on the number of bars spliced and size of the specimens tested. Available test data seem to indicate that a splice in a wide section could be considered stronger than a similar splice in a beam containing only a small number (one or two) of spliced bars. The added strength of splices in a wall could be attributed to the fact that a smaller percentage of splices in a wall section are edge splices.

Therefore, the basic questions are: (1) What are the behavior patterns of wall-type spliced sections? (2) Would the alteration or elimination of the edge splices in such a section lead to a significant increase in strength of the wall splice? (3) How much would transverse reinforcement in the splice region of a wide section affect the strength of the section? (4) How well do splice strength equations predict the performance of wall section splices?

CHAPTER 2

TEST PROGRAM

2.1 Description of Specimens

Twenty-five tests were conducted to study reinforcing bar splice behavior in wide sections. The tests were proportioned to simulate a cantilever retaining wall. Figure 2.1 compares the prototype and the model. In a typical retaining wall, the splice would be vertically cast and would be subjected to a moment gradient with only one end of the splice subjected to maximum moment. All test specimens were subjected to a two-point loading to produce a constant moment along the splice. With uniform moment the splice is subject to a stress condition as severe as that in the prototype. Previous studies[1,2] indicate that the strength of the splice subjected to different stresses at the ends can be related to the strength under uniform stress. Previous tests[1] indicate that diagonal tension failures may be triggered by a splice bond failure in specimens subjected to a variable moment with no stirrup reinforcement in the critical region. Therefore, the tests of specimens without transverse reinforcement are difficult unless uniform moment (no shear) is applied. Therefore, the two-point loading system described later in this chapter was chosen for the twenty-five tests.

In an attempt to bound the condition of vertically cast bars in the prototype, two of the test specimens contained top cast bars, with the remaining twenty-three containing bottom cast bars. All specimens were rested in the position shown in Fig. 2.1, with the tension face upright for observation during testing.

2.1.1 Specimen Geometry and Details. Of the twenty-five specimens tested, one contained #6 bars, ten had #8 bars, ten had #11 bars, and four contained #14 bars. Specimen side views are shown in Figs. 2.2 and 2.3. The laboratory test floor had an anchor bolt pattern on a 4 ft. spacing.

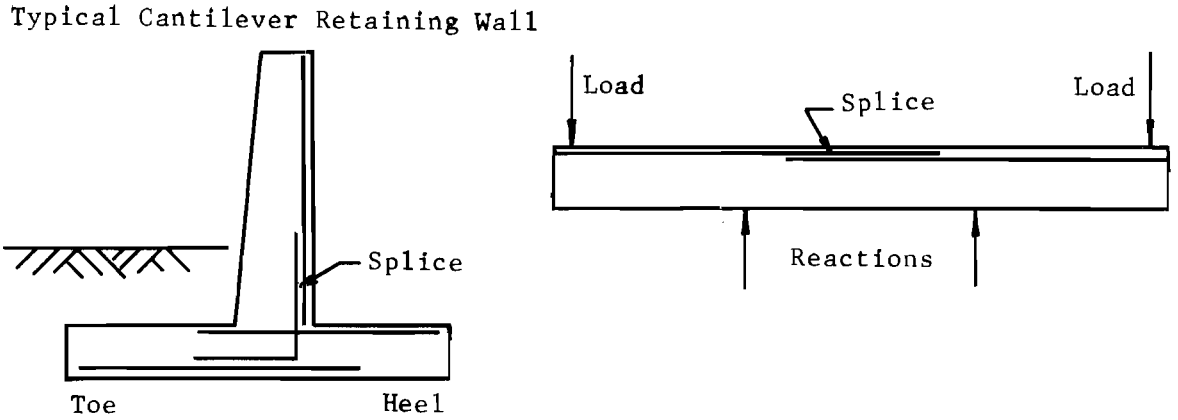

Fig. 2.1. Prototype and model

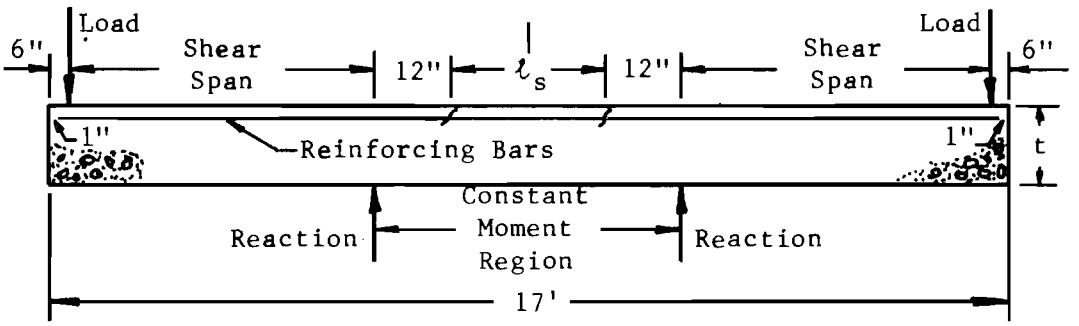

Fig. 2.2. Side view of #6, #8, and #11 bar specimens

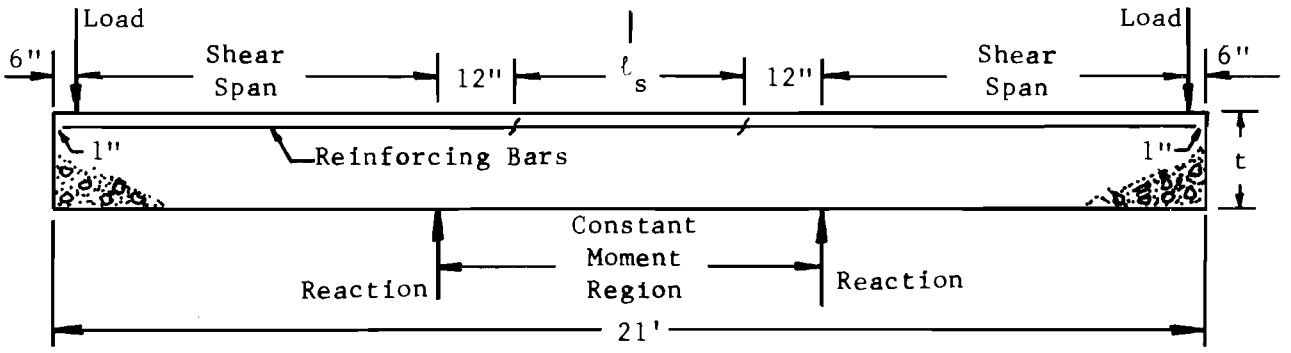

Fig. 2.3. Side view of #14 bar specimens

The loading was applied 6 in. from the end of the specimen. This resulted in an overall specimen length for the #14 bar specimens of 21 ft., with smaller bar specimens having an overall length of 17 ft. The reactions were located 12 in. outside the ends of the splices. With varying splice lengths (ℓ_s) and constant specimen lengths, the shear span was varied between specimens.

Figures 2.4 to 2.6 show typical cross sections for the various test beams. The overall depth of beams with bottom cast bars was chosen to ensure yielding could occur before a compression failure resulted, provided a splice failure did not occur first. In specimens with top cast bars, the overall depth was chosen so at least 12 in. of concrete were cast below the bars.

Quantitative details of the twenty-five test specimens are summarized in Table 2.1. The notation used in this table to identify each of the tests is explained by the sample shown below:

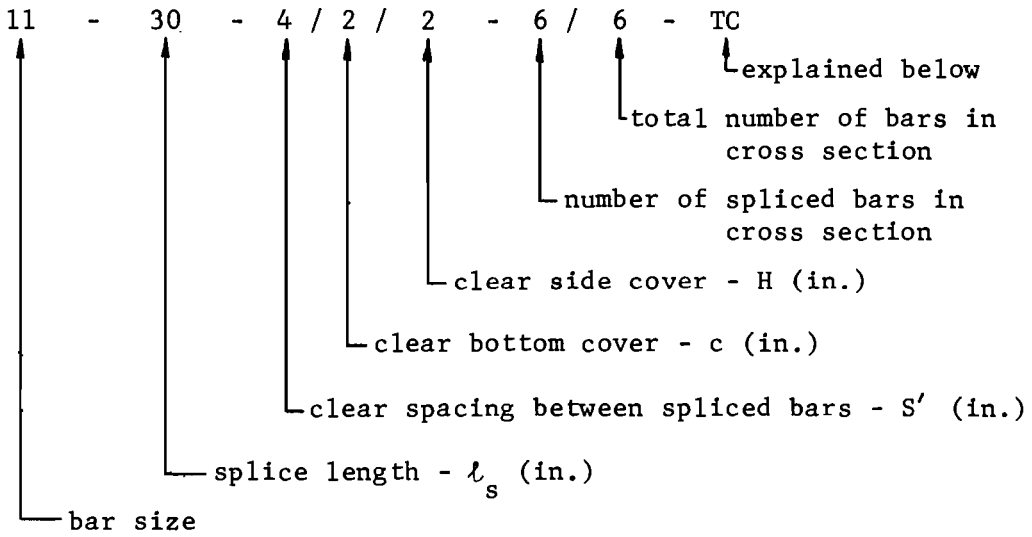

The final letters or digits, if needed, signify top cast bars (TC), spiral reinforcement in the splice region (SP), or #3 stirrups in the splice region and the nominal spacing of these stirrups (S5, for example, signifies #3 stirrups at 5 in.).

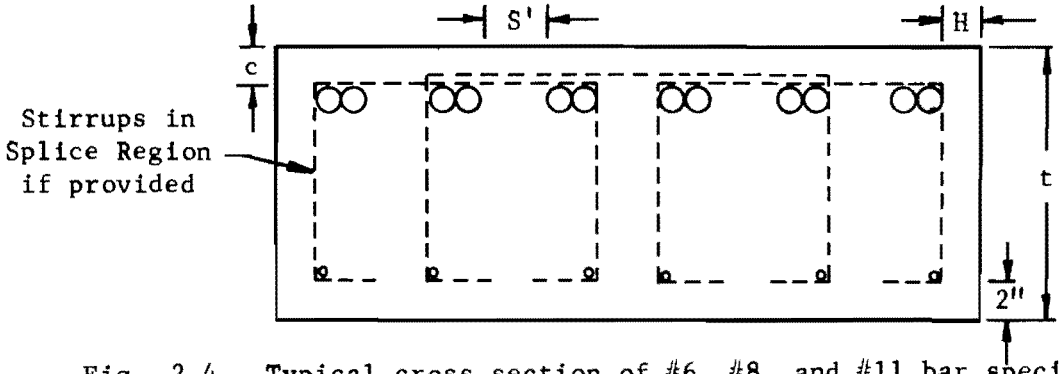

Fig. 2.4. Typical cross section of #6, #8, and #11 bar specimens with all bars spliced (shown in testing position)

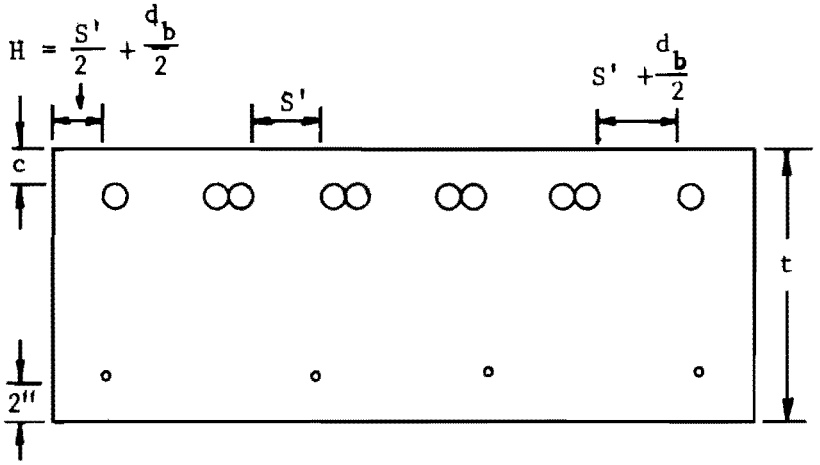

Fig. 2.5. Typical cross section of #8 and #11 bar specimens with continuous edge bars (shown in testing position)

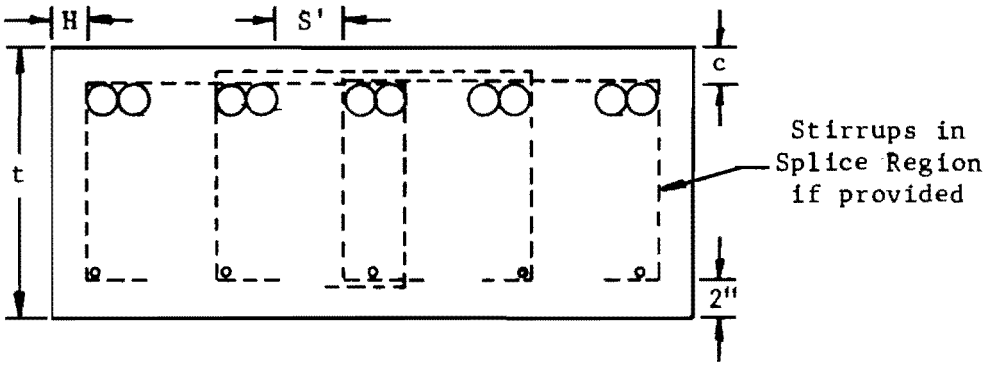

Fig. 2.6. Typical cross section of #14 bar specimens (shown in testing position)

TABLE 2.1. DETAILS OF TEST SPECIMENS

Specimen	Cross-section Properties										Steel Strengths		Transverse Reinforcement			Member Lengths				Concrete Properties		
	d_b in.	No. of Spliced Bars	Total No. of Bars	S' in.	c in.	H in.	t in.	b in.	d in.	ρ %	f_y ksi	f_{yt} ksi	Effective Stir.Spcg. in.	Actual Stir.Spcg. in.	ρ_t %	Specimen Length ft.	ℓ_s in.	Constant Moment Region in.	Shear Span in.	f'_c psi	f'_t psi	Age at Test (days)
6-12-4/2/2-6/6	0.75	6	6	4.0	2.0	2.0	13.0	33.0	10.625	0.75	61.7	---	---	---	---	17.0	12.0	36.0	78.0	3731	486	65
8-18-4/3/2-6/6	1.00	6	6	4.0	3.0	2.0	13.0	36.0	9.5	1.39	59.3	---	---	---	---	17.0	18.0	42.0	75.0	4710	---	46
8-18-4/3/2.5-4/6	1.00	4	6	4.0	3.0	2.5	13.0	36.0	9.5	1.39	59.3	---	---	---	---	17.0	18.0	42.0	75.0	2920	374	27
8-36-4/1/2-6/6	1.00	6	6	4.0	1.0	2.0	13.0	36.0	11.5	1.14	59.3	---	---	---	---	17.0	36.0	60.0	66.0	2525	363	40
8-36-4/1/2.5-4/6	1.00	4	6	4.0	1.0	2.5	13.0	36.0	11.5	1.14	59.3	---	---	---	---	17.0	36.0	60.0	66.0	3440	440	27
8-36-4/1/4-6/6	1.00	6	6	4.0	1.0	4.0	13.0	40.0	11.5	1.03	59.3	---	---	---	---	17.0	36.0	60.0	66.0	2910	386	24
8-24-4/2/2-6/6	1.00	6	6	4.0	2.0	2.0	13.0	36.0	10.5	1.25	59.3	---	---	---	---	17.0	24.0	48.0	72.0	3105	388	33
8-24-4/2/2.5-4/6	1.00	4	6	4.0	2.0	2.5	13.0	36.0	10.5	1.25	59.3	---	---	---	---	17.0	24.0	48.0	72.0	3375	406	45
8-24-4/2/4-6/6	1.00	6	6	4.0	2.0	4.0	13.0	40.0	10.5	1.13	59.3	---	---	---	---	17.0	24.0	48.0	72.0	3760	408	46
8-15-4/2/2-6/6-S5	1.00	6	6	4.0	2.0	2.0	13.0	36.0	10.5	1.25	61.1	65.5	5.0	6.0	0.367	17.0	15.0	39.0	76.5	3507	434	61
8-24-4/2/2-6/6-TC	1.00	6	6	4.0	2.0	2.0	16.0	36.0	13.5	0.98	55.7	---	---	---	---	17.0	24.0	48.0	72.0	2640	333	30
11-45-4/1/2-6/6	1.41	6	6	4.0	1.0	2.0	13.0	40.875	11.295	2.03	60.5	---	---	---	---	17.0	45.0	69.0	61.5	3520	445	37
11-30-4/2/2-6/6	1.41	6	6	4.0	2.0	2.0	13.0	40.875	10.295	2.22	60.5	---	---	---	---	17.0	30.0	54.0	69.0	2865	380	30
11-30-4/2/4-6/6	1.41	6	6	4.0	2.0	4.0	13.0	44.875	10.295	2.03	63.4	---	---	---	---	17.0	30.0	54.0	69.0	3350	452	57
11-30-4/2/2.7-4/6	1.41	4	6	4.0	2.0	2.7	13.0	40.875	10.295	2.22	66.3	---	---	---	---	17.0	30.0	54.0	69.0	4420	544	62
11-25-6/2/3-5/5	1.41	5	5	6.0	2.0	3.0	13.0	44.063	10.295	1.72	66.3	---	---	---	---	17.0	25.0	49.0	71.5	3920	448	67
11-20-4/2/2-6/6-S5	1.41	6	6	4.0	2.0	2.0	13.0	40.875	10.295	2.22	67.3	67.3	5.0	6.0	0.323	17.0	20.0	44.0	74.0	3400	433	68
11-20-4/2/2-6/6-S2.9	1.41	6	6	4.0	2.0	2.0	13.0	40.875	10.295	2.22	67.3	67.3	2.86	3.0	0.565	17.0	20.0	44.0	74.0	3620	406	52
11-30-4/2/2-6/6-S5	1.41	6	6	4.0	2.0	2.0	13.0	40.875	10.295	2.22	65.0	68.0	5.0	5.0	0.323	17.0	30.0	54.0	69.0	3063	385	20
11-20-4/2/2-6/6-SP	1.41	6	6	4.0	2.0	2.0	13.0	40.875	10.295	2.22	67.3	64.0	3.0 (pitch)	---	0.244	17.0	20.0	44.0	74.0	3263	412	71
11-30-4/2/2-6/6-TC	1.41	6	6	4.0	2.0	2.0	16.0	40.875	13.295	1.72	67.0	---	---	---	---	17.0	30.0	54.0	69.0	2907	377	26
14-60-4/2/2-5/5	1.693	5	5	4.0	2.0	2.0	16.0	37.5	13.154	2.28	57.7	---	---	---	---	21.0	60.0	84.0	78.0	2865	369	65
14-60-4/2/4-5/5	1.693	5	5	4.0	2.0	4.0	16.0	41.5	13.154	2.06	57.7	---	---	---	---	21.0	60.0	84.0	78.0	3197	369	73
14-40-4/2/2-5/5-S3	1.693	5	5	4.0	2.0	2.0	16.0	37.5	13.154	2.28	57.7	66.5	3.08	3.0	0.572	21.0	40.0	64.0	88.0	3010	350	83
14-40-4/2/2-5/5-S5.7	1.693	5	5	4.0	2.0	2.0	16.0	37.5	13.154	2.28	57.7	66.5	5.71	6.0	0.308	21.0	40.0	64.0	88.0	3500	416	124

2.1.2 Variables. (1) Splice Length and Bar Diameter. For a given bar size, an estimation of the required splice length was made using both ACI recommendations [3] and proposals by Ferguson and Krishnaswamy [2]. Using this information, a splice length was selected such that a splice failure was expected before the steel yielded. Previous tests [1] indicated that once the bars yield larger deformations associated with yielding may change the failure pattern. On specimens with transverse reinforcement the splice length was reduced even further to account for the beneficial influence of the transverse reinforcement. Thus, the splice length varied from 12 in. for a #6 splice to 60 in. for #14 splices without stirrup reinforcement.

(2) Ratio of Clear Bottom Cover to Clear Spacing of Splices. Other studies [1,2, and 4] have shown that the required length of a lapped splice is dependent upon the clear cover and clear spacing of the spliced bars. It becomes convenient to express these parameters in the form of a ratio of the clear bottom cover to the clear spacing between the splices.

The clear spacing between the spliced bars was maintained at 4 in. for all tests, except for one specimen with #11 bars which had a clear spacing of 6 in. The clear bottom cover was varied from 1 in. for several of the #8 and #11 bar specimens, to 3 in. for two of the #8 bar specimens. Thus, the ratio of C/S' varied from 0.25 to 0.75.

(3) Edge Condition. Previous studies [2] have indicated that in the case where a number of bars are spliced at the same section, the failure of the splice may be initiated by splitting near the edge or outside splice. Therefore, the influence of the outside edge splices on the strength of the splice was a main variable in the test program. In a beam section containing a number of bars spliced at the same section, the outside edge splices may be critical and reduce the strength of the section as a whole. In a wide wall section, the edge splices may be a small percentage of the total number of splices. The effect of edge splices may not be as pronounced in these wider sections as in a beam section containing perhaps two splices both of which are edge splices.

For the wide specimens tested in this program, the number of edge splices to total number of splices was either 2 to 5, or 2 to 6.

The possibility of increasing the strength of the outside edge splice was studied. In specimens with all bars spliced, the clear edge cover was equal to one-half the clear spacing in seventeen tests and in four tests was equal to the clear spacing. In four tests, the outside edge bar was continuous. With continuous edge bars, the clear edge cover and the first inside clear spacing increased by the dimension of a bar radius over the identical fully spliced sections (see Fig. 2.5).

(4) Transverse Reinforcement. Previous work [1,2] noted that transverse reinforcement around a splice increased the splice strength and also resulted in a less brittle failure. Seven specimens contained transverse reinforcement, six with U-stirrups and one with spiral reinforcement.

The percentage of stirrup reinforcement supplied in the splice region varied for the tests from 0.31 to 0.57 percent. All stirrups were fabricated using #3 bars. For specimens with #8 and #11 bars containing transverse reinforcement in the splice region, each splice was at the corner of a stirrup (see Fig. 2.4). For specimens with #14 bars with transverse reinforcement, the middle splice had two corners providing confinement, while the remaining spliced bars in the section had one corner providing confinement (see Fig. 2.6).

One specimen with #11 splices contained spiral reinforcement in the splice region around the lapped splices. Spiral reinforcement extended beyond the ends of the lap splice for a distance of 6-1/2 in. at each end of the lap. The internal diameter of the 1/4 in. plain spiral was 4-1/4 in., with a pitch of 3 in. A spiral was used to confine each splice with no other transverse reinforcement employed in the splice region.

(5) Casting Position. Pullout tests [5] have shown that anchorage strength of bars cast horizontally is adversely affected by the accumulation of water and air beneath a bar due to the bleeding of the mix. The

greater the depth of concrete below the bar, the greater the accumulation beneath the bar. Currently, for top cast bars with greater than 12 in. of concrete cast below, the splice length must be increased by 40 percent.

In a typical retaining wall, the splice is cast in a vertical position. Vertical casting of test specimens was ruled out because of size and handling problems. Bottom cast specimens are likely to match the bond characteristics of a vertically cast splice in a wall quite closely; however, two specimens were top cast in order to bound the problem. The specimens were cast with more than 12 in. of concrete below the bars and were identical to other tests which contained bottom cast bars with only overall depth of the beam increased to allow 12 in. of concrete to be cast below the bars.

(6) Concrete Strength. Although not a prime variable, the compressive strength of the ready-mix concrete varied from test to test. For the twenty-five tests, the compressive strength of the concrete varied from 2525 psi to 4710 psi.

2.1.3 Materials. (1) Concrete. All specimens were cast with ready-mix concrete, using Type I cement, and Colorado River sand and gravel. The maximum size of aggregate used was 3/4 in. Ideally, the water-to-cement ratio was 0.65. The slump varied considerably with each test. The mix was designed to yield a compressive strength of 3500 psi. The measured average strength was 3440 psi. The average compressive concrete strength for each test is shown in Table 2.1, along with the age of the specimen at testing.

(2) Steel. Because of the number of specimens and the various bar sizes used, the steel used in the specimens arrived in different shipments. All steel exhibited a well-defined yield point. Coupon tests of all bars were loaded until yielding had occurred. Loading was then stopped, and the yielding was allowed to proceed with no additional loading of the material. After about five minutes, the load which the coupon maintained was recorded as the static yield load of the material. With this method the effect of the method of loading and test machine size

on the yield point of the steel was minimized. The modulus of elasticity of the steel was about 29,000 ksi for all tests.

2.1.4 Instrumentation. Strain gage instrumentation was employed in all tests to determine steel stresses in the bars. Gaging of the lapped splice bars followed one of three regular patterns shown in Appendix 1. Gaging of stirrup reinforcement in the splice region is also shown in Appendix 1.

All strain gages had a gage length of 1/4 in. The strain gage installation procedure was as follows: one bar deformation was ground off at the position of the gage to produce a clear spacing between lugs of about 1 in. The loss of metal due to this process was negligible. The surface was filed, sanded, and cleaned with acetone. The surface was prepared for the strain gage mounting with a metal conditioner and a neutralizer. The gages were attached with epoxy and allowed to cure at least 24 hours. After attaching lead wires, the strain gage and lead connection was waterproofed using a polymer-rubber pad and coated with a silicone rubber sealer.

2.1.5 Fabrication of Specimens. The main tension reinforcement was cut to length. Following usual construction practice, rust or mill scale was not removed from the bars. The bars were lap spliced, with saw cut ends heading into the splice. About ten tie wires were used to hold each lap together. Care was taken to ensure that the strain gages were placed so any bending of the bars would not prejudice the gage reading.

For all tests, transverse reinforcement in the shear spans was designed to ensure that a shear failure did not occur before a flexural or splice failure could occur in the constant moment region. The transverse reinforcement extended the entire length of the shear span in all specimens. For specimens without stirrup reinforcement in the splice region, transverse reinforcement in the shear span did not extend into the constant moment region. For specimens with stirrup reinforcement along the splice, the transverse reinforcement in the shear spans extended to within a stirrup spacing of the ends of the lapped bars.

For the specimen with spiral reinforcement in the splice region, the transverse reinforcement in the shear spans did not extend into the constant moment region of the specimen.

All but two of the specimens were cast and transported with the main steel in the bottom of the specimen. To control cracking which might develop during removal of the specimen from the form and placement in the loading frame, a small amount of top longitudinal steel was used, as shown in Figs. 2.4 through 2.6. This compression steel also helped position the transverse reinforcement.

The specimens were cast in adjustable wooden forms. The forms were adequately braced to maintain dimensions under the weight of the fresh concrete. For bottom cast specimens, chairs were used at the bottom and sides to control concrete cover. No chairs were used in the splice zone. In specimens with top cast bars, the cage was hung from supports across the forms with heavy wire in order to control cover and chairs were used on the sides.

Lifting inserts were secured to the cage at the quarter points for hoisting purposes. The location of lifting points was selected to reduce the possibility of tension cracking in the splice region during transport.

Specimens were cast using ready-mix concrete. The ready-mix concrete was checked and water added as necessary to obtain an acceptable slump. Concrete was cast in two lifts using the chute of the concrete truck. The concrete was compacted using a mechanical vibrator. Twelve standard 6 × 12 in. cylinders were cast with each specimen. They were compacted by internal vibrating with a small mechanical vibrator. The tops of the beams and cylinders were screeded and troweled smooth. The complete casting operation took about an hour.

After the concrete had set, the specimen and the cylinders were covered with a polyethelene sheet. After one or two days, the specimen and the cylinders were stripped and allowed to cure side by side in the laboratory.

At the time of testing, the specimens were moved with the use of an overhead crane. Bottom cast specimens were turned over so that the splice tension face would be upright during testing. The specimen was moved to the reaction pedestals, where it was centered and aligned. The specimen was raised a small amount above the pedestals using four mechanical jacks. Reaction rollers and plates were positioned, and the plates were grouted to the specimen. The loading plates on each end were also grouted. The loading frame was placed on the loading plates, resting on a second set of rollers. The frame was centered and adjusted. At this point, the dead weight of the specimen and of the loading frame was being carried by the mechanical jacks. Strain gage positions in the splice region were marked on the surface for reference. Lead wires from the strain gages were checked for continuity and connected to the data acquisition system. Finally, beam dimensions in the splice region were measured.

2.2 Specimen Loading System

2.2.1 Description of Constant Moment Loading System. The loading system and test setup is shown in Figs. 2.7 through 2.9. All specimens were subjected to a two-point loading, producing a constant moment region along the splice with no shear. The loading was applied by four hydraulic rams, of either 30 or 60 ton capacity, depending upon the requirements of the test. Each of these rams was placed between a plate, which was anchored to the floor with four bolts, and a lower reaction beam. Each lower reaction beam carried the load from two rams. The load from the lower reaction beam was transferred to an upper reaction beam through four 1 in. diameter, 5 ft. long, loading bolts at each end of the specimen. The load from the loading bolts to the upper and lower reaction beams was transferred through four sections of 4 × 4 in. tubing, each cut to accommodate two of the loading bolts. The specimen was loaded by the upper reaction beam through a roller assembly and plate which had been previously grouted in place.

An electric pump operating through a four-way manifold loaded the rams. The level of the load was always measured in three ways. A 10,000 psi pressure transducer located at the pump measured hydraulic line pressure. A 100 kip load cell was used at each ram to check the actual

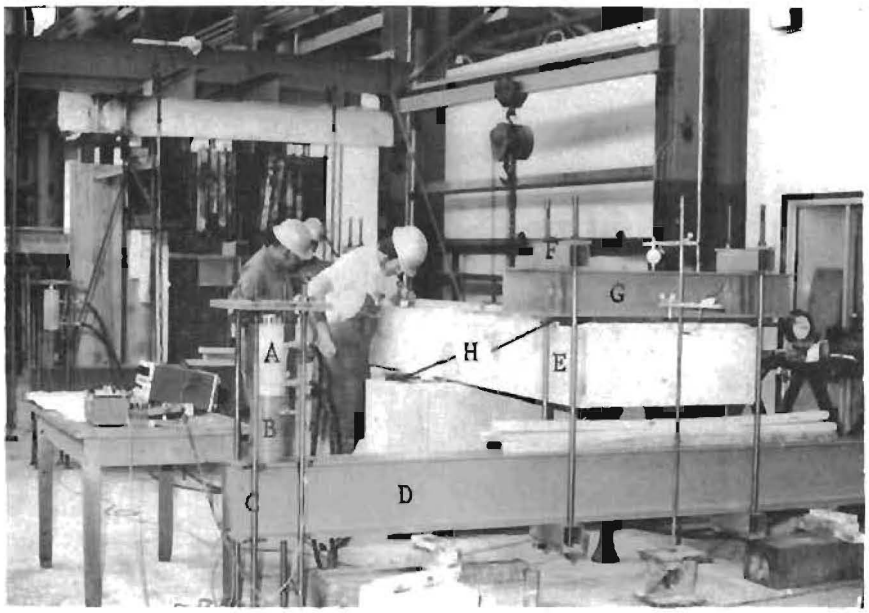

A. Hydraulic Ram
B. Load Cell (2)
C. Floor Bolts
D. Lower Reaction Beam
E. Loading Bolts
F. 4 x 4 inch Tubing
G. Upper Reaction Beam
H. Roller and Plate Assembly

Fig. 2.7. Loading frame and specimen during testing.

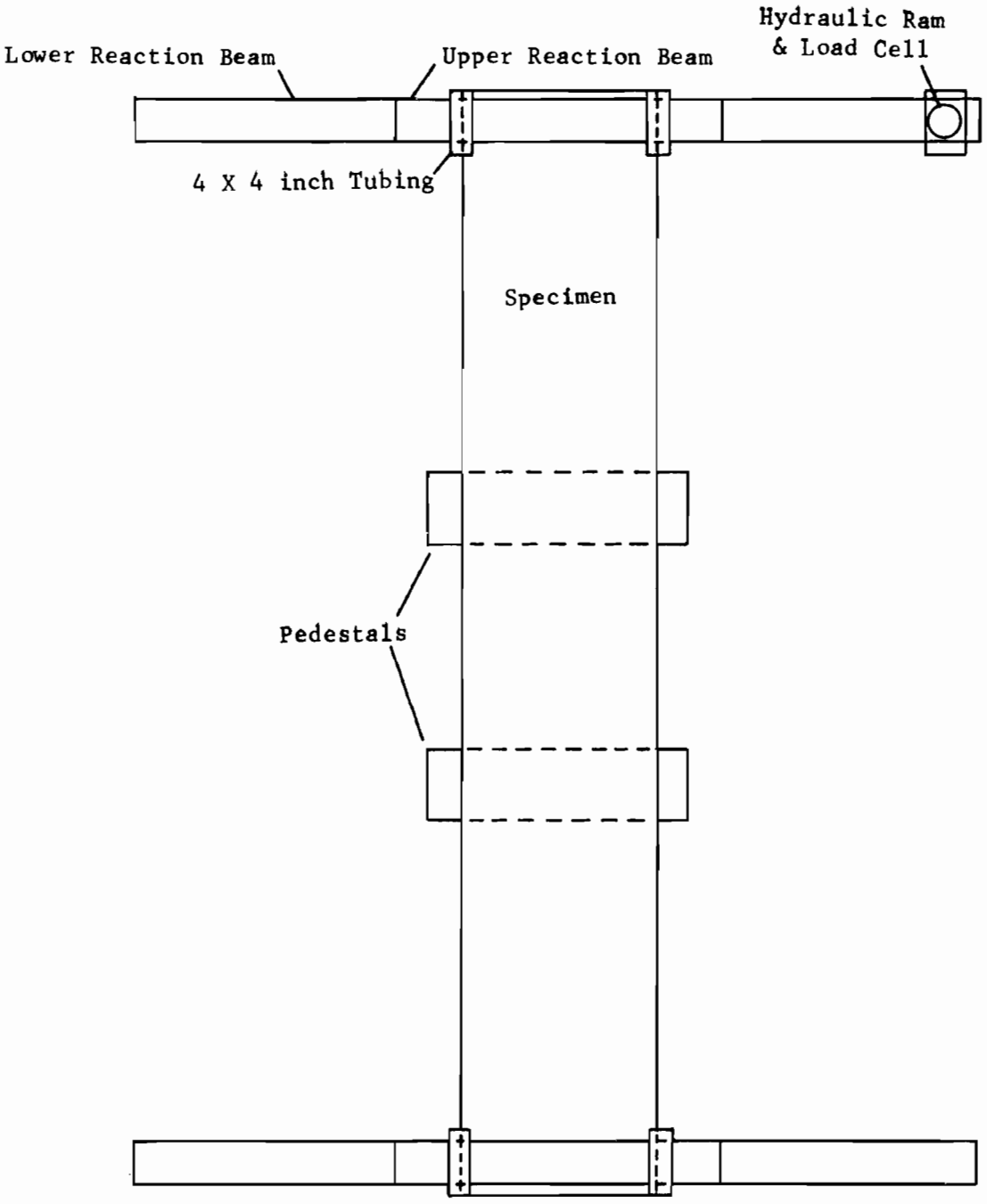

Fig. 2.8. Plan view of loading frame and specimen

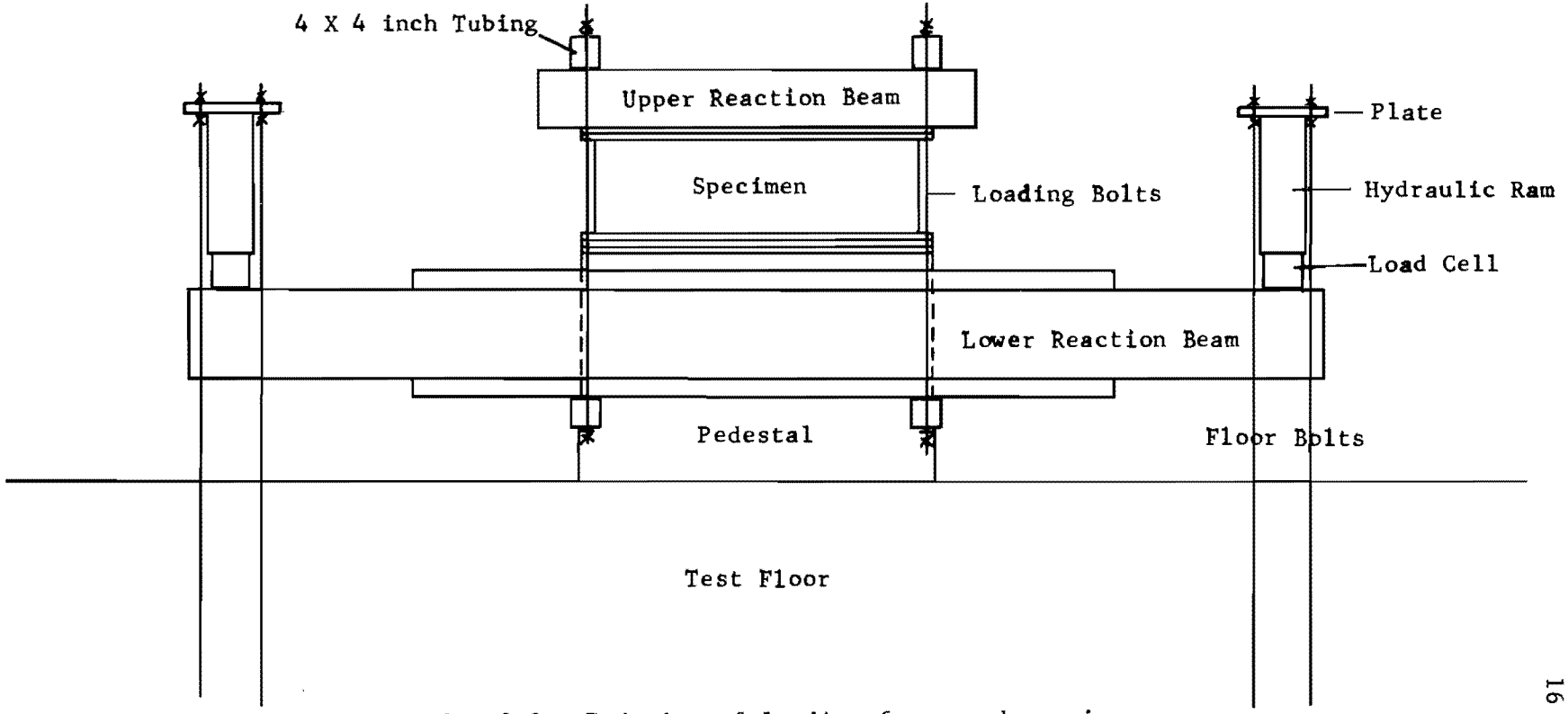

Fig. 2.9. End view of loading frame and specimen

load distribution. As a backup to the pressure transducer, a calibrated 10,000 psi pressure gage was also monitored at the pump.

2.2.2 Dead Loadings on the Specimens. The specimen was resting on mechanical jacks, which supported the weight of the beam and the loading frame, at the start of the test. The jacks were removed for the first load stage. For the purpose of analysis, the dead weight of the specimen and loading frame was expressed as an equivalent applied load at the loading points on the specimen. This point loading was selected to produce the same dead load moment at the ends of the splice as was produced by the distributed dead load of the specimen and the point load of the loading frame. This equivalent dead load ranged from 4 to 13 percent of the total load. A tabulation of the equivalent dead loads is shown in Appendix 2.

2.3 Test Procedure

Most data recording was accomplished using a rapid data acquisition system. The system recorded all data on magnetic tape which was later reduced using a computer program developed for this purpose, and also provided a printed copy of the data at the time of the test. All strain gages, load cells, and deflection potentiometer readings were recorded.

Dial gages and deflection potentiometers were used at each end and at the middle of the specimen to record deflection readings of the specimen. The dial gages were used to monitor the deflection of the specimen during the test.

The loading was applied progressively in predetermined increments until signs of splitting distress occurred. At this point, the loading increment was reduced, and the specimen was loaded to failure. It normally took a few minutes for the load to stabilize at high loads.

All pertinent data were collected after each load increment. The widths of flexural cracks on the tension face at the splice region were measured with a crack measuring microscope at various load levels. The least count of the microscope was 0.001 in. Cracks on the tension

face and sides of the specimen were marked and the load at which they occurred was labeled alongside. After failure had occurred, the failure surfaces were photographed from various angles.

CHAPTER 3

TEST RESULTS AND OBSERVATIONS

The behavior of lapped splices in wide sections can be evaluated by observation of the cracking patterns on the failure surfaces, the level of strain (or stress) in the steel in the splice region, and the final failure modes of the specimens. The progression of splitting in the splice region traced the pattern of failure in the splice, with areas under greatest distress showing the largest amount of splitting. Strain distributions across the splice end and along the splice length were produced. In general, a close correlation between the cracking patterns, steel strain distributions, and failure modes of the specimens was exhibited.

3.1 Cracking Patterns and Failure Modes

The first cracks to appear in the specimens tested were flexural cracks. Since the stresses in the bars were greatest at the ends of the splice, flexural cracking occurred at this location first and the cracks at the splice ends were the widest flexural cracks in the constant moment region. As the loading was increased on the specimen, flexural cracking progressed from the splice ends deeper into the splice. Outside of the splice, flexural cracking occurred at about evenly spaced intervals throughout the constant moment region. Flexural cracking also occurred in the shear spans of the specimen.

Splitting cracks in the vicinity of the splice led to the failure of a specimen. As described in Ref. [1], differential strains between spliced bars at a given section along a lap splice result in slip between the bars and the surrounding concrete. At low loads, the concrete distress associated with stress transfer is concentrated at the ends of the splice. With increased loading, the stress between bars is transferred along a greater length of the lap. With sufficiently high stresses in the bars, distress in the concrete results in cracking or splitting near the ends of

the splice. As cracking becomes visible on the surfaces of a specimen, the progression of cracking leading to failure can be observed. Failure of a specimen occurs when cover on the splices is lost due to splitting over a substantial length of the splice. The failure is normally fairly brittle when a splice fails.

The following modes of failure were observed in the specimens tested in this program.

(1) Face and Side Split - Figure 3.1 shows a diagram of the face and side split failure for a wide section containing several spliced bars. For specimens failing in this mode, initial splitting occurred in the clear cover over the edge splices. As splitting cracks developed on the sides, the edge "block" would tend to break loose, destroying the bond along the outside edge splices. The remaining interior splices failed in a face split mode. This mode of failure normally occurred for specimens having an edge cover of one to two clear cover thicknesses.

(2) Confined Face Split Mode - Specimens which either used edge cover greater than two clear cover thicknesses or continuous edge bars failed in the confined face split mode. This failure geometry is shown in Fig. 3.2. As in specimens with smaller edge cover, the first splitting cracks in the splice region appeared over the edge splices. Because the edge cover was wide and relatively stiff, splitting cracks did not form on the sides of a specimen. Failure resulted in a lifting of the clear cover between the edge splices, and the resulting loss of bond for the splices.

(3) Face Split Mode - Figure 3.3 diagrams the face split failure for a specimen in which the edge cover was less than the clear cover. The clear cover over the splices exhibited no splitting distress prior to failure. The first sign of splitting distress appeared as side splitting cracks when failure was imminent. As the splitting in the horizontal plane through the splices became extensive, the cover on the tension face lifted with no longitudinal cracking in the cover.

V-type failures noted in previous splice tests [1,2] were not observed in this series of tests because the spacing to cover ratio was generally too small for this to occur.

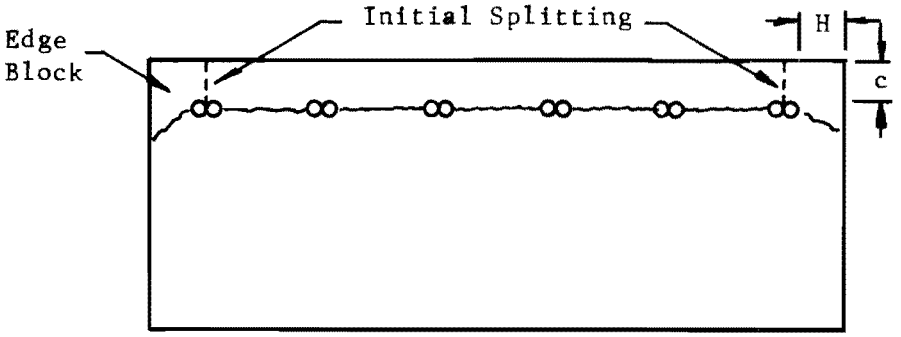

Fig. 3.1. Face and Side Split Failure Mode ($c \leq H \leq 2c$)

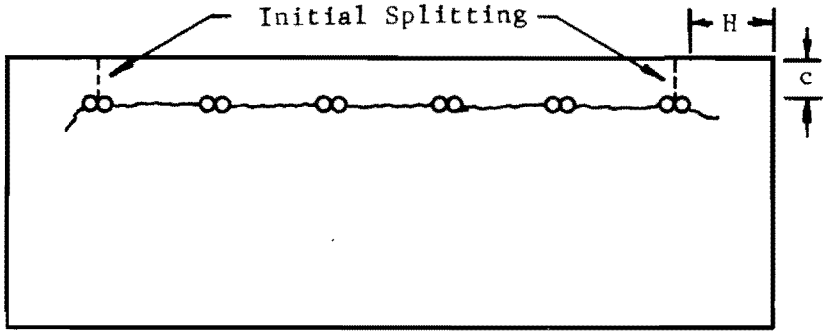

Fig. 3.2. Confined Face Split Failure Mode ($H > 2c$)

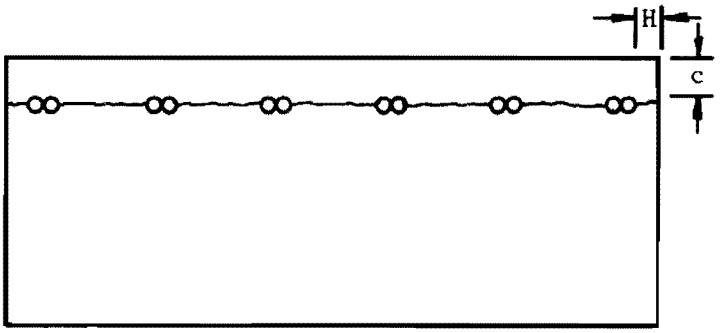

Fig. 3.3. Face Split Failure Mode ($H < c$)

The mode of failure of each of the twenty-five specimens is given in Table 3.1. For the purpose of discussing cracking patterns and failure modes of the specimens, it becomes convenient to discuss the following groups of specimens exhibiting similar behavioral patterns.

3.1.1 All Bars Spliced. Fourteen specimens contained splices in which all the bars were lap spliced, and no transverse steel was present in the splice region. Twelve were bottom cast, and two were top cast. In general, specimens with all bars spliced exhibited the greatest splitting distress. The thickness of the clear cover and side cover seemed to govern the cracking patterns and failure modes of the specimens. It is possible to group the specimens with all bars spliced according to the ratio of side cover (H) to clear cover (c) for the specimens.

(1) Side cover equal to one or two clear cover thicknesses ($1 \leq H/c \leq 2$). Figures 3.4 through 3.9 show typical failure surfaces for specimens having an edge cover that was about equal to the clear cover over the bars. Ten specimens fall into this general category, with all exhibiting similar behavior.

The first sign of splitting distress appeared as fine splitting cracks near the ends of the splice on the tension face. The splitting cracks appeared on the outside edge splices initially, and with increased loading, also appeared on the interior splices. As the load level increased, the splitting distress progressed along the splice. The tension surface splitting occurred both along and inclined to the length of the splice (see Fig. 3.6). The inclined cracks likely were due to a redistribution of internal stresses from exterior to interior splices once the cover on the exterior splices split and the capacity of the splice was reduced.

Near ultimate load, splitting cracks also appeared on the sides of the specimens (see Fig. 3.7). The appearance of side splitting usually indicated failure was imminent. The failure was usually sudden and brittle, with wide cracks opening on the surface.

TABLE 3.1. TEST RESULTS

SPECIMEN	DESCRIPTION OF FAILURE	ULTIMATE LOAD (kips)	f_s (load) (ksi)	f_s (gages) (ksi)	f_s (edge) (ksi)	AVERAGE CRACK WIDTH at f_s = 36 ksi (inches)	MAXIMUM CRACK WIDTH MEASURED (inches)
6-12-4/2/2-6/6	Face and Side Split	18.6	57.3	55.9-E	46.4-E	0.012	0.022
8-18-4/3/2-6/6	Face Split	29.7	56.2	57.9	51.2	0.019	0.034
8-18-4/3/2.5-4/6	Confined Face Split	25.7	49.3	45.4	45.3	0.019	0.033
8-36-4/1/2-6/6	Face and Side Split - Yielding	39.4	54.6	59.3-Y	46.7	0.007	0.021
8-36-4/1/2.5-4/6	Flexural - Steel Yielded	47.4	59.3-Y	59.3-Y	59.3-Y	0.008	0.022
8-36-4/1/4-6/6	Confined Face Split - Yielding	45.6	59.3-Y	59.3-Y	59.3-Y	0.008	0.023
8-24-4/2/2-6/6	Face and Side Split	30.6	50.6	53.5	51.3	0.012	0.020
8-24-4/2/2.5-4/6	Confined Face Split - Yielding	37.6	59.3-Y	59.3-Y	59.3-Y	0.012	0.028
8-24-4/2/4-6/6	Face and Side Split - Yielding	40.8	59.3-Y	59.3-Y	59.3-Y	0.012	0.028
8-15-4/2/2-6/6-S5	Face and Side Split	32.7	57.3	54.1	41.3	0.013	0.018
8-24-4/2/2-6/6-TC	Face and Side Split	38.9	49.6	47.7	27.8	0.022	0.031
11-45-4/1/2-6/6	Face and Side Split	66.4	45.3	44.4	37.9	0.013	0.022
11-30-4/2/2-6/6	Face and Side Split	44.7	37.9	39.4	33.6	0.018	0.025
11-30-4/2/4-6/6	Face and Side Split	52.8	44.4	44.1	40.5	0.017	0.028
11-30-4/2/2.7-4/6	Confined Face Split	68.7	57.5	55.3-E	55.3-E	0.016	0.029
11-25-6/2/3-5/5	Face and Side Split	42.9	44.2	40.0	28.7	0.015	0.019
11-20-4/2/2-6/6-S5	Face and Side Split	44.8	40.6	35.0	26.7	0.013	0.018
11-20-4/2/2-6/6-S2.9	Face and Side Split	46.8	42.3	42.1	37.6	0.014	0.027
11-30-4/2/2-6/6-S5	Face and Side Split	54.8	46.3	45.0	35.6	0.011	0.014
11-20-4/2/2-6/6-SP	Face and Side Split	46.8	42.4	41.3-E	26.1	0.014	0.024
11-30-4/2/2-6/6-TC	Face and Side Split	57.1	36.9	33.4-E	28.2-E	0.016*	0.018
14-60-4/2/2-5/5	Face and Side Split	73.0	45.7	44.6-E	40.9-E	0.024	0.028
14-60-4/2/4-5/5	Face and Side Split	91.3	56.6	53.8	49.2	0.021	0.036
14-40-4/2/2-5/5-S3	Flexural - Steel Yielded	85.4	57.7-Y	57.7-Y	57.7-Y	0.008	0.009
14-40-4/2/2-5/5-S5.7	Face and Side Split - Yielding	87.4	57.7-Y	57.7-Y	48.6	0.013	0.021

E - Extrapolated Point
Y - Yield Stress of Longitudinal Steel
* - Measured at f_s = 30 ksi

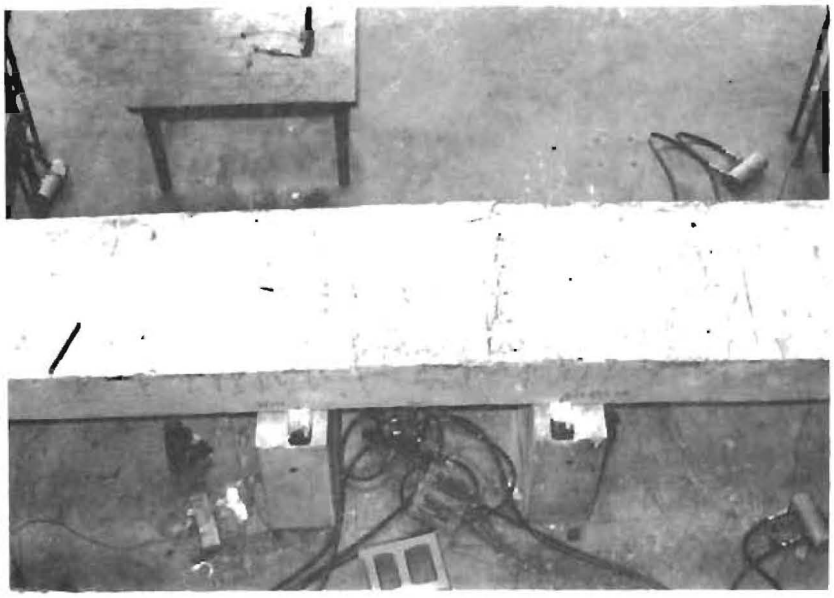

Fig. 3.4. Tension face of 8-24-4/2/2-6/6 after failure

Fig. 3.5. Side view of 8-24-4/2/2-6/6 after failure

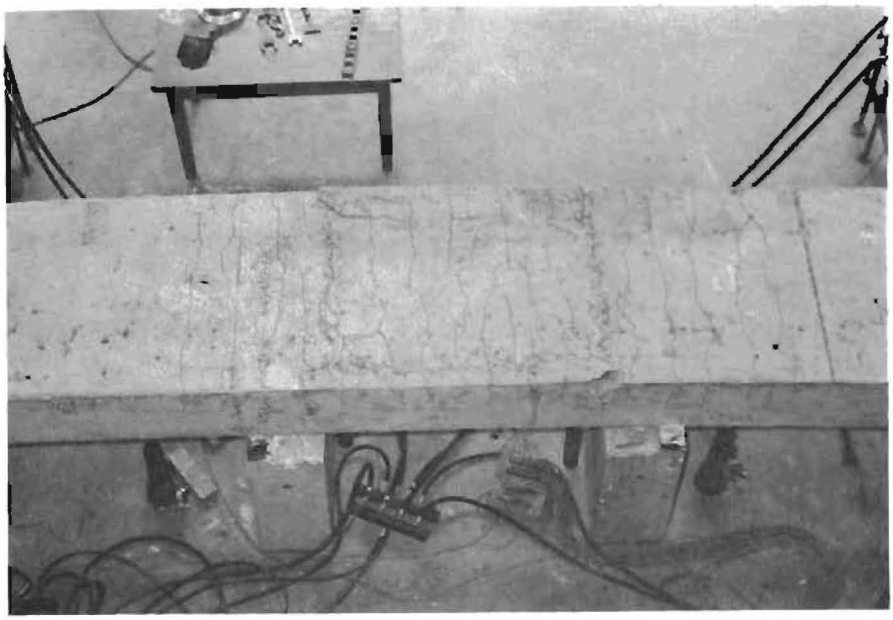

Fig. 3.6. Tension face of 11-45-4/1/2-6/6 after failure

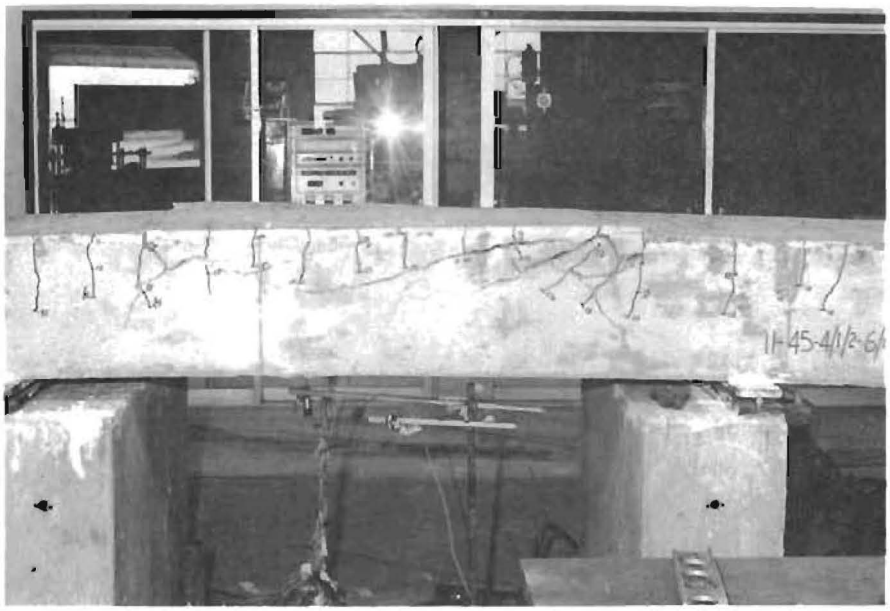

Fig. 3.7. Side view of 11-45-4/1/2-6/6 after failure

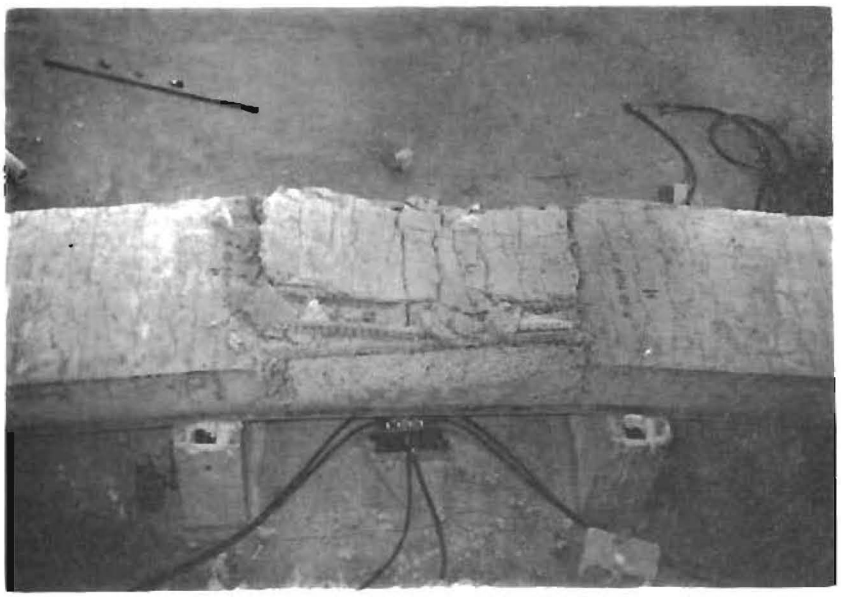

Fig. 3.8. Tension face of 14-60-4/2/4-5/5 after failure

Fig. 3.9. Side View of 14-60-4/2/4-5/5 after failure

The edge splices in this group of specimens normally exhibited greater distress than interior splices. The first splitting cracks on the tension face opened along the edge splices and progressed well along the splice before similar splitting cracks appeared above the interior splices (see Fig. 3.6). As side splitting cracks formed on the specimen, the strength of the edge splices deteriorated, and stresses in the interior splices increased. When splitting spread to the interior splices, failure of the entire splice region occurred.

The face and side split failure mode (see Fig. 3.1) correlates with the progression of cracking indicated above. The formation of the edge "block" denoted the loss of bond of the outside edge splices. The remaining interior splices failed with a general lifting of the clear cover over the bars (see Fig. 3.9).

(2) Side cover much greater than clear cover ($H/2 > 2$). One test, 8-36-4/1/4-6/6, had side cover of four times the clear cover thickness. The crack patterns at failure for this specimen are shown in Figs. 3.10 and 3.11.

The first signs of distress appeared as splitting cracks on the tension face. However, in contrast with tests having smaller edge cover, side splitting cracks did not appear on the specimen (see Fig. 3.11). Failure was confined to the tension face, with the edge "block" remaining intact while the cover over the interior bars continued splitting. Upon failure of the specimen, the clear cover over the interior bars tended to lift as a unit (see Fig. 3.11).

As with specimens having smaller edge cover, the edge splices in the section exhibited the greatest splitting distress during loading. Splitting cracks on the tension face seemed to progress throughout the length of the edge bars, but because the edge cover was wide and relatively stiff, splitting cracks did not form on the sides of the specimen. This resulted in the confined face split mode of failure for this test (see Fig. 3.2).

(3) Side cover less than clear cover ($H/C < 1$). One test, 8-18-4/3/2-6/6, had side cover which was equal to half the clear cover

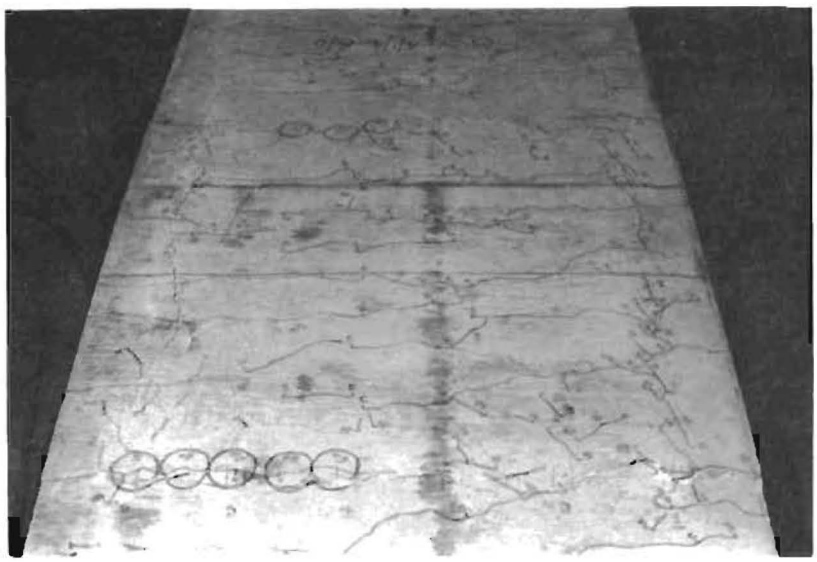

Fig. 3.10. Tension face of 8-36-4/1/4-6/6 after failure

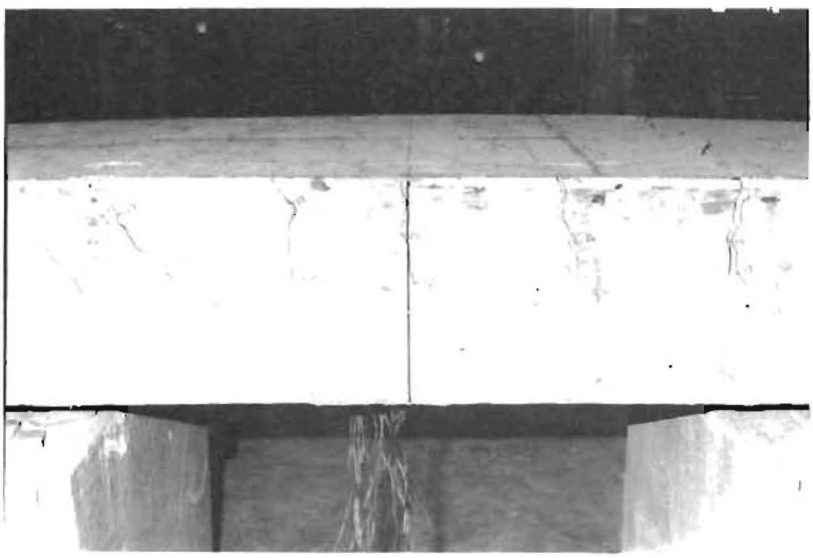

Fig. 3.11. Side view of 8-36-4/1/4-6/6 after failure

of the specimen. The failure surfaces for this specimen are shown in Figs. 3.12 and 3.13.

As loading increased, the tension surface exhibited no splitting distress prior to failure. The first sign of distress appeared as side splitting near the ends of the splice when failure was imminent. When failure occurred, the side cover split along the entire length of the splice, with the cover over all of the bars lifting up as a unit (see Fig. 3.12).

It seems reasonable to assume splitting in the vicinity of the outside edge splices was extensive prior to failure, but this is difficult to determine by examination. Side splitting cracks appeared on the specimen prior to failure, but it is impossible to determine if similar splitting was occurring around the interior splices. Because the clear cover was thick and relatively stiff, splitting cracks did not form on the tension surface prior to failure. The resulting failure mode was a face split failure (see Fig. 3.3).

3.1.2 Continuous Edge Bars. Four specimens were tested with all interior bars spliced and the two outside edge bars continuous. No transverse reinforcement was used in the splice section. In general, cracking was contained much better for these specimens as compared to specimens with all bars spliced, and splice performance in general was improved.

Figures 3.14 and 3.15 show typical failure surfaces for a specimen employing continuous edge bars. As expected, the edge splices showed no splitting on the tension or side faces. Some splitting cracks appeared over interior splices, with cracking normally starting on the interior splices next to the continuous edge bars. The splitting appeared to be more uniformly distributed over the interior splices than in other tests with all bars spliced (see Fig. 3.14). In general, side splitting cracks were not a problem in specimens with continuous edge bars (see Fig. 3.15). The failure mode of these specimens would be classified as the confined face split (see Fig. 3.2).

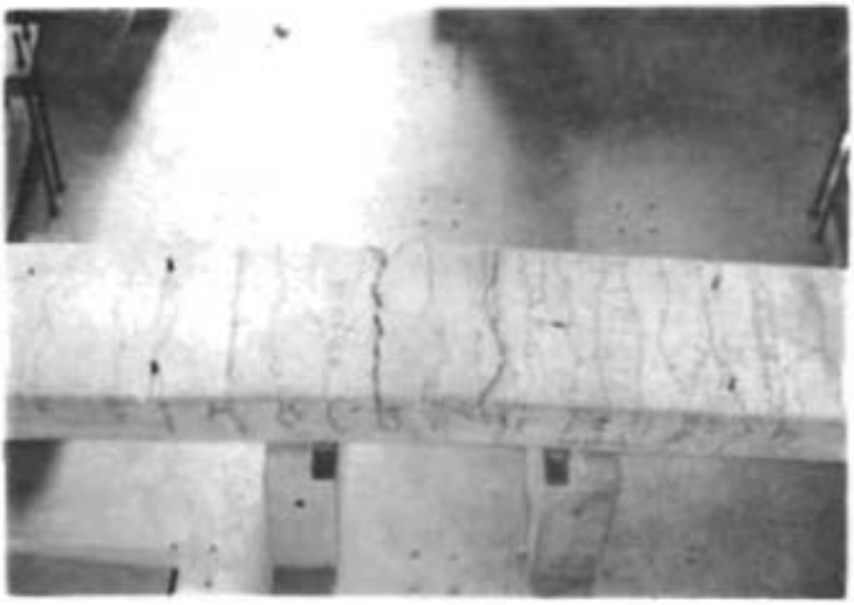

Fig. 3.12. Tension face of 8-18-4/3/2-6/6 after failure

Fig. 3.13. Side view of 8-18-4/3/2-6/6 after failure

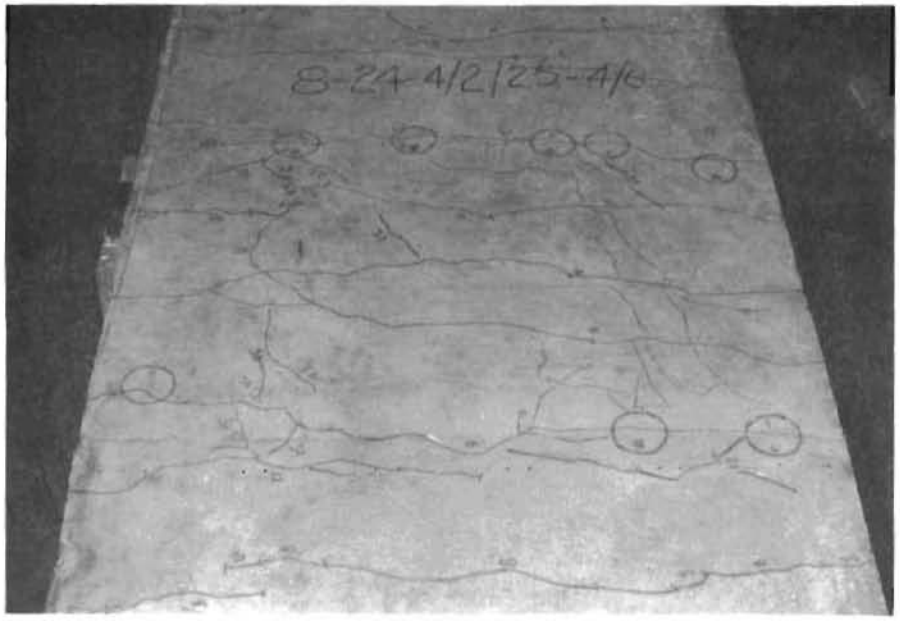

Fig. 3.14. Tension face of 8-24-4/2/2.5-4/6 after failure

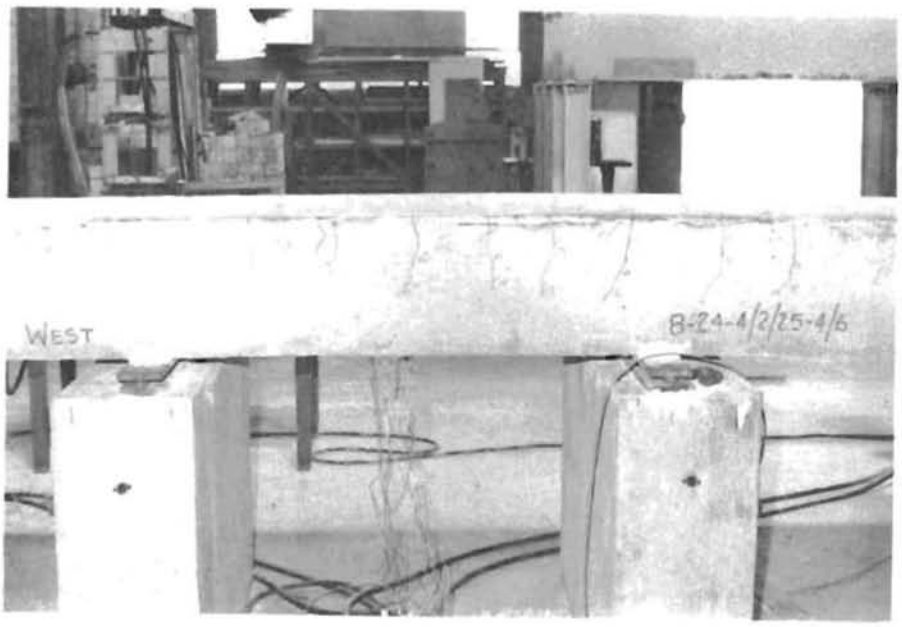

Fig. 3.15. Side view of 8-24-4/2/2.5-4/6 after failure

3.1.3 Splices with Transverse Reinforcement. Seven specimens contained transverse reinforcement, six with U-stirrups and one with spiral reinforcement. Several of these specimens failed by splitting of the concrete. The condition of a typical specimen at failure is shown in Figs. 3.16 and 3.17.

Cracking of specimens containing transverse reinforcement was much less severe than that of specimens without transverse reinforcement. The presence of the transverse reinforcement seemed to distribute cracking more evenly throughout the splice (see Fig. 3.16). Splitting was restrained by the transverse reinforcement with no wide cracks or severe separation of cover occurring at failure. The presence of transverse reinforcement did not seem to influence the mode of failure of a specimen, provided a splice failure occurred. The seven specimens with transverse reinforcement failed in the face and side split mode (see Fig. 3.1).

3.2 Steel Stresses

3.2.1 Average Stresses in Longitudinal Steel. To verify the accuracy of strain gage readings recorded during testing, it was necessary to compare the measured or observed stresses in the reinforcing steel to the stresses calculated from the total applied load.

Using a cracked transformed section for a given specimen, a linear relationship can be obtained between the total applied moment (or load) and the average steel stress in the reinforcing steel at the section. It is assumed that the concrete carried no tension, and that the relationship between the compressive stress and strain in the concrete is linear.

In order to determine stresses in the reinforcing steel, all the bars in the cross section at one end of the splice were instrumented (see Appendix 1). Using strain measurements, the average steel stress across the section can be determined for a given load (or moment) applied to the specimen.

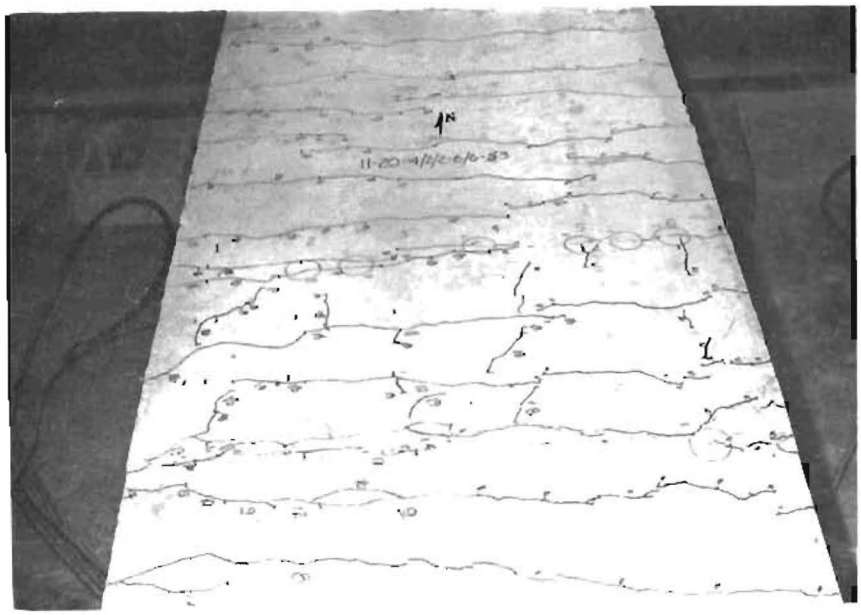

Fig. 3.16. Tension face of 11-20-4/2/2-6/6-S3 after failure

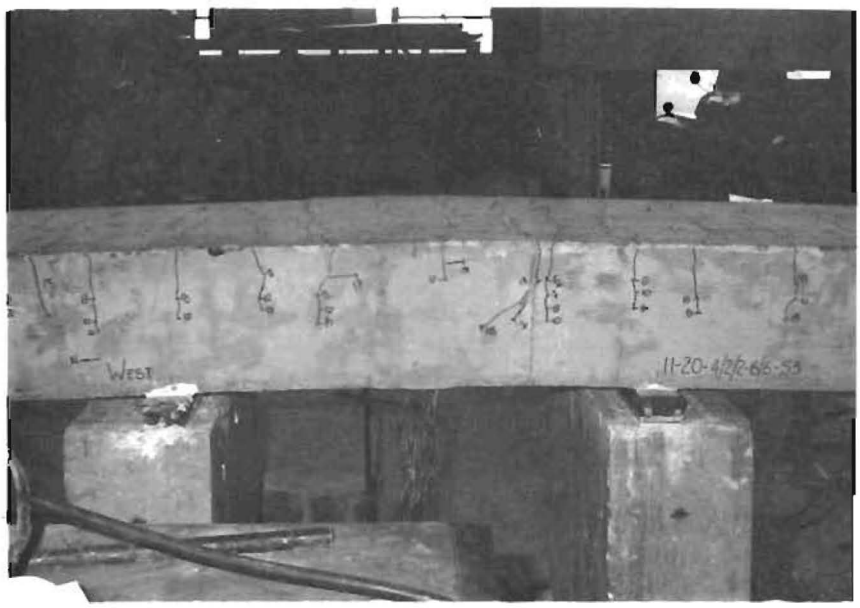

Fig. 3.17. Side view of 11-20-4/2/2-6/6-S3 after failure

Typical plots of the load versus average bar stress are shown in Figs. 3.18 and 3.19. The load includes the dead weight of the specimen and the loading frame. Using a cracked transformed section, the bar stress calculated from total loads is a straight line. On the same figure, the average bar stress obtained from the strain gage readings is plotted for various levels of total loading.

At low levels, the difference between the observed and the calculated bar stress is fairly significant. At higher loads and higher bar stresses (approaching yield), the difference decreases. The divergence of the observed and calculated curves at low loads is due mainly to the assumption of cracked section properties. At low loads, the section is uncracked, and steel stresses are relatively low because the concrete is carrying tension which may be a significant portion of the total tensile force on the cross section. At higher stress levels, the concrete cracks and the tensile capacity of the concrete is insignificant compared to the tensile force present in the steel. Thus, the calculated and measured stresses tend to agree more closely.

Table 3.1 gives the values of the calculated and observed average bar stresses at failure for each of the test specimens. The agreement is generally good, however, there is some experimental scatter in the results. In general, the strain gages accurately monitored the strains in the reinforcing bars, and may be used for further analysis.

3.2.2 Bar Strains across End of Splice. In order to understand the behavior of the test specimens, a study of the distribution of strain across the end of the splice will help to illustrate differences in the performances of exterior or edge splices and interior splices. Appendix 1 shows gage locations on the longitudinal steel for this comparison.

Figures 3.20 through 3.24 show strain distributions in the longitudinal steel across the end of the splice at various load levels for five different specimens. Steel strains are plotted rather than steel stresses. With yielding, the steel stress remains constant but the strain may change and provide a better indication of the behavior of the splice.

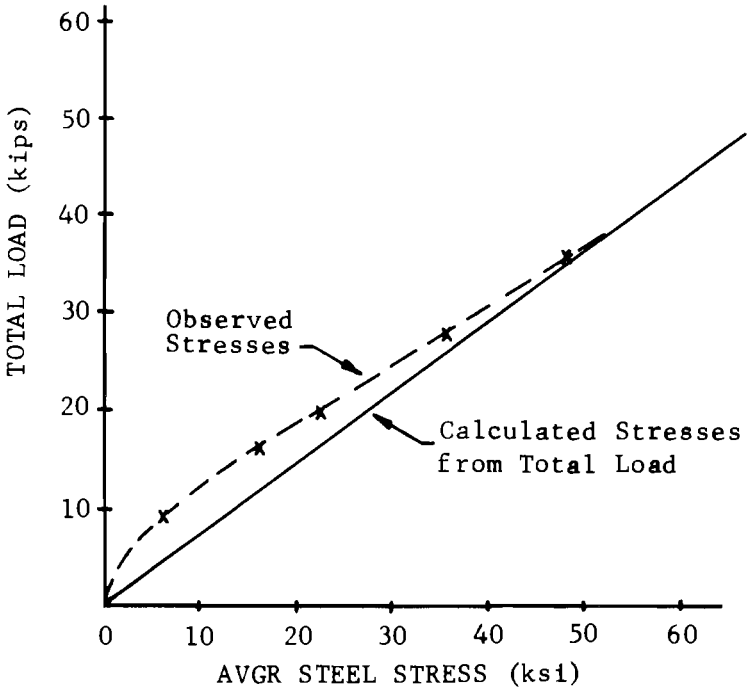

Fig. 3.18. Load versus steel stress for 8-36-4/1/4-6/6

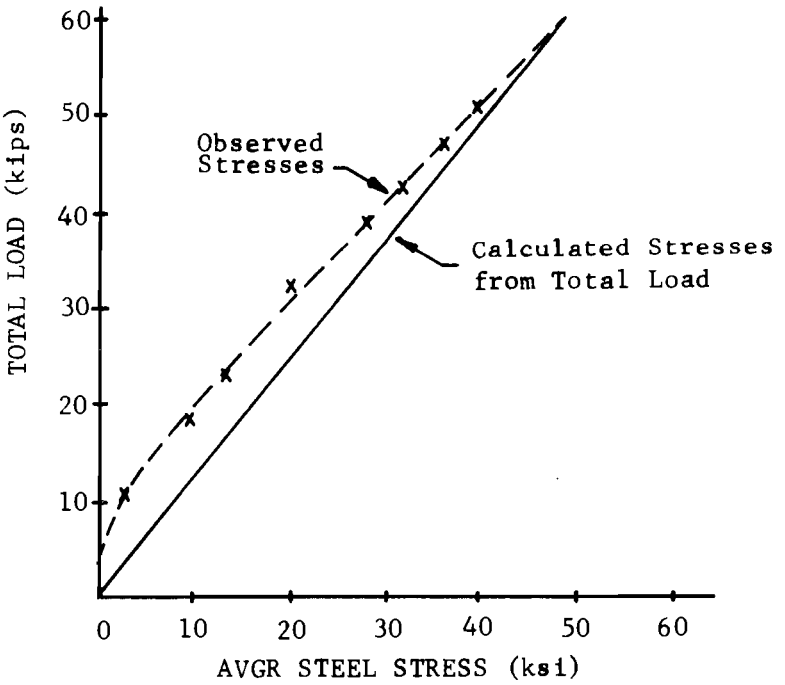

Fig. 3.19. Load versus steel stress for 11-30-4/2/4-6/6

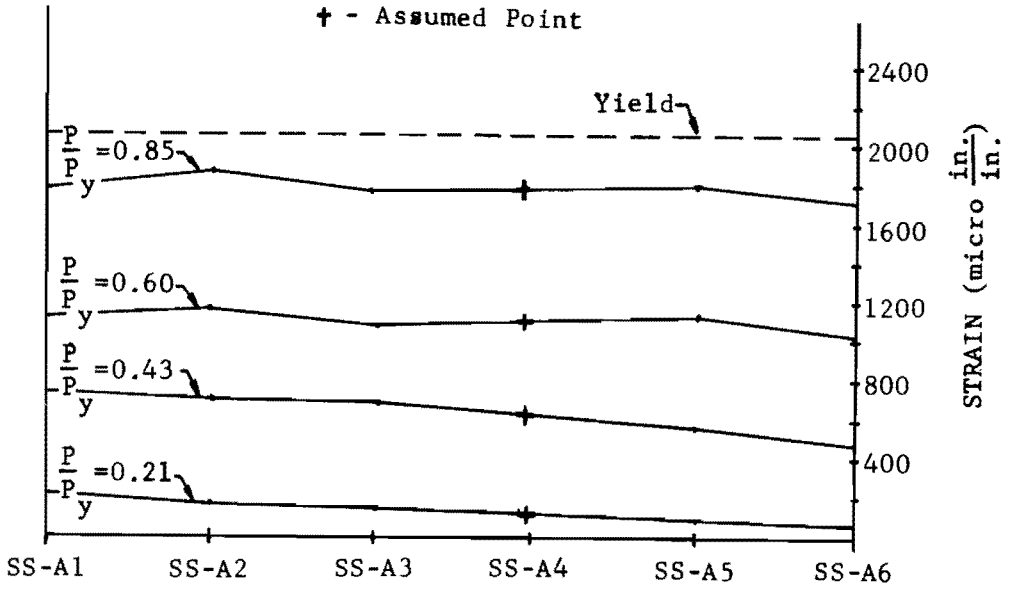

Fig. 3.20. Steel strain distribution across splice end of specimen 8-24-4/2/2-6/6 (face and side split failure)

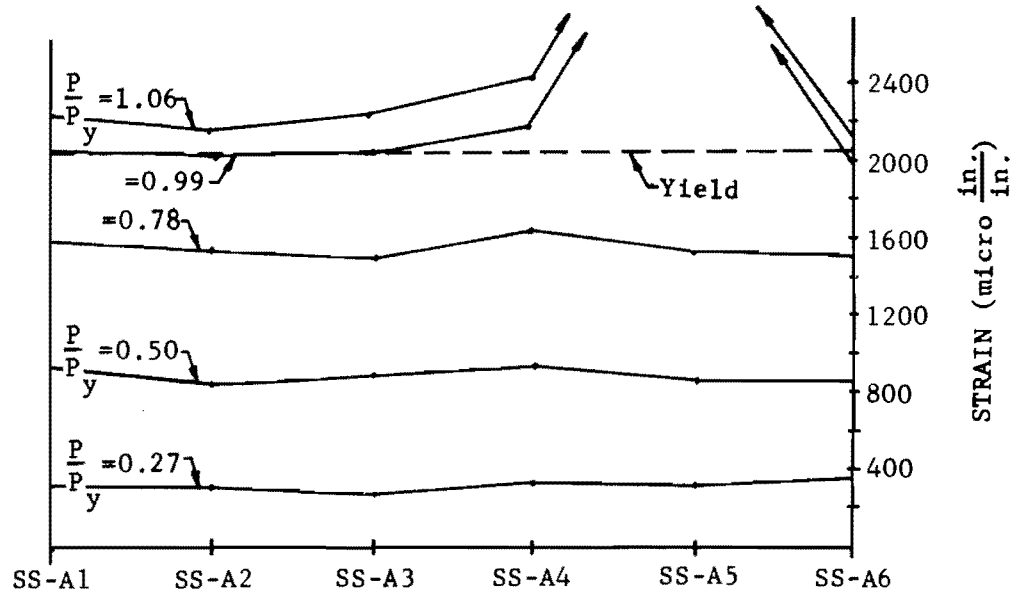

Fig. 3.21. Steel strain distribution across splice end of specimen 8-36-4/1/4-6/6 (confined face split failure)

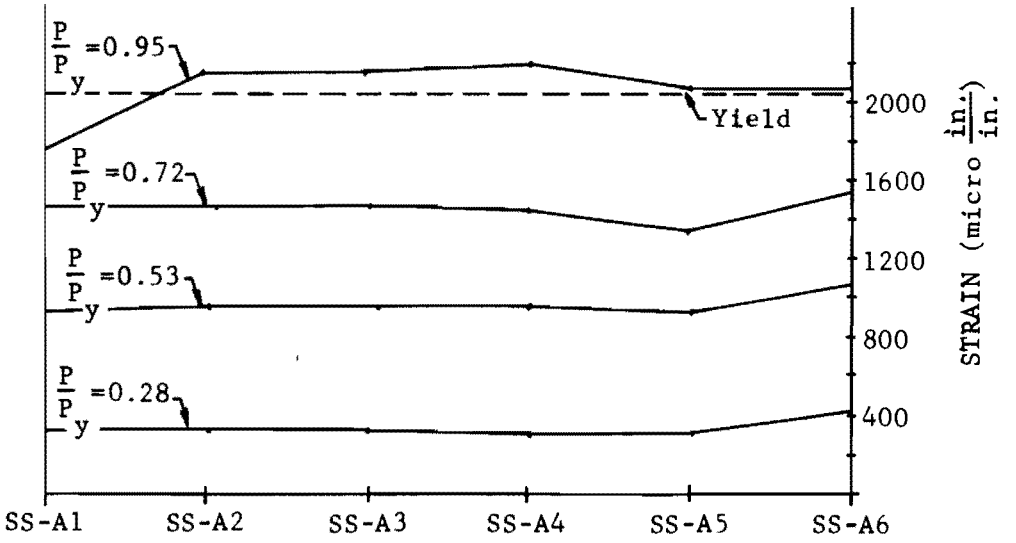

Fig. 3.22. Steel strain distribution across splice end of specimen 8-18-4/3/2-6/6 (face split failure)

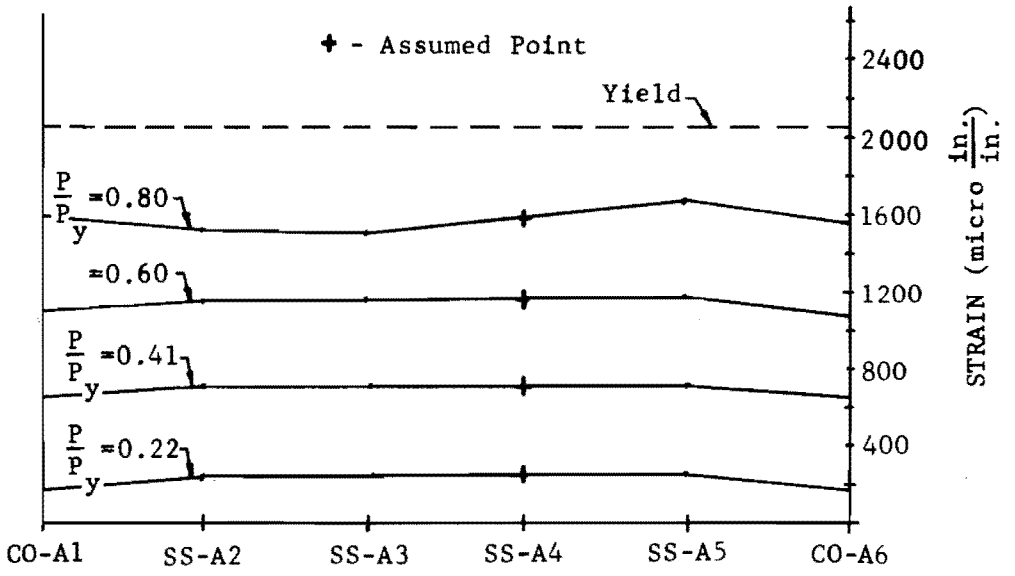

Fig. 3.23. Steel strain distribution across splice end of specimen 8-18-4/3/2.5-4/6 (continuous edge bar)

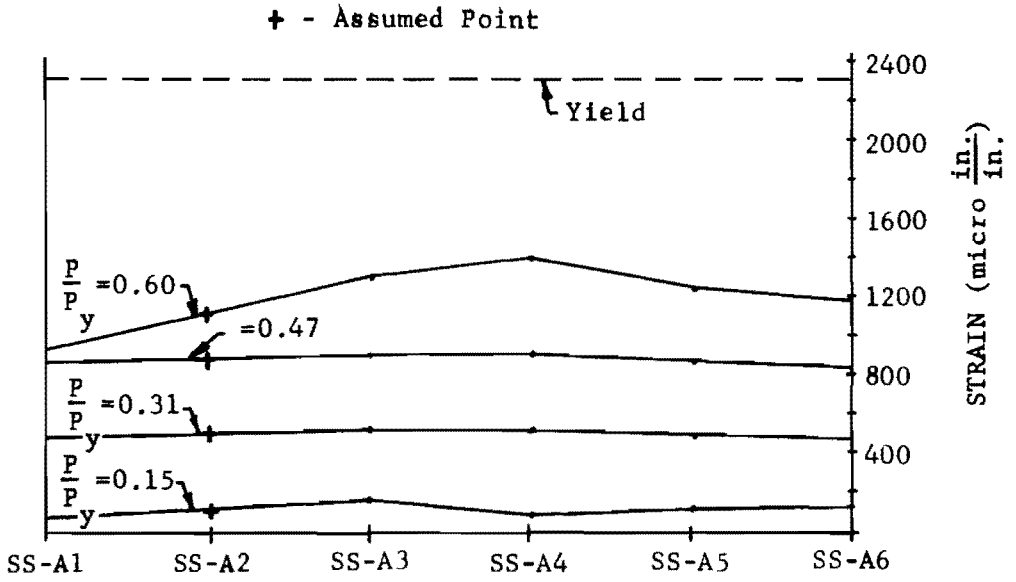

Fig. 3.24. Steel strain distribution across splice end of specimen 11-20-4/2/2-6/6-S5 (stirrup reinforcement present in splice region)

Each curve is plotted for a selected load level expressed as a ratio of the total applied load (including the dead weight of the specimen and the loading frame) to the load required to yield the bars (P_y). The value of the yield load was calculated using a cracked transformed section. In some cases curves are shown for $P/P_y > 1.0$ which may be attributed to the linear analysis used. In other cases it may be due to experimental errors in loads or strains. However, for purposes of comparison, the yield load based on a cracked transformed section was deemed sufficiently accurate.

Figure 3.20 shows typical strain distributions across the splice end section for a specimen with all bars spliced which failed in the face and side split mode. At low loads, the strain distribution across the section is relatively uniform. As load is increased, the strain distribution becomes less uniform, with the edge bar strains slightly less than exterior bar strains. It is also noted that generally the first interior splices seem to be picking up the load not carried by the edge bars, with the remaining interior splices exhibiting nearly identical strains. At failure, strains in the edge splices are definitely less than those in the interior bars.

The strain distributions shown relate directly to the failure pattern described for the specimen. Generally for the face and side split mode of failure, the edge splices showed the greatest cracking and splitting distress. The loss of capacity associated with splitting is evident in the strain distributions, because the edge splices are at lower strains (or stresses) than the interior splices.

Figure 3.21 shows the steel strain distributions across the splice end section for the specimen with all bars spliced which failed in the confined face split mode of failure. For all load levels, the strain distributions across the section remain relatively uniform. The failure of the specimen was such that the clear cover over all of the bars was the critical factor in the splice strength, and the edge cover was thick enough that the edge splices were not weakened. This fact is

reflected in the strain distributions across the section, in that it shows the edge splices performing as well as the interior splices up to yield.

Figure 3.22 shows the steel strain distributions for the specimen with all bars spliced which failed in the face split mode of failure. The strain distribution across the section remained fairly uniform until failure of the specimen occurred. Because the strain dropped off rapidly in the edge splice at location SS-A1, it seems reasonable to assume that failure of the specimen initiated at this point. At a ratio of $P/P_y = 0.72$, the strains are uniform across the section. However, at $P/P_y = 0.95$, the strain at one edge bar dropped markedly. The progression of splitting in the specimen corresponds with the strain behavior in that the appearance of side splitting cracks triggered failure of the specimen.

Figure 3.23 shows the strain distributions across the splice end section for a typical specimen containing continuous edge bars. The strain distributions for these specimens is generally similar to the distributions in the specimen which had a large edge cover and failed in the confined face split mode (see Fig. 3.21). The agreement between the strain distributions for the specimens with continuous edge bars and the specimen with large edge cover is supported by the fact that with continuous edge bars, the specimens tended to fail in the confined face split mode of failure over the interior splices.

The presence of transverse reinforcement, stirrups or spirals, in the splice region did not seem to affect the distributions of steel strain, as shown in Fig. 3.24. This correlates with the observation that the addition of transverse reinforcement in the splice region did not seem to alter the failure mode of a specimen.

The strain distributions of the two specimens with top cast bars did not vary significantly from similar bottom cast specimens. Weaker bond characteristics of the top cast splices did not seem to affect the strain distributions, however, the strength of the splices was reduced.

In comparing failure modes and strain distributions across the splice ends for the twenty-five tests, it is clear the mode of failure of the specimens directly influences the shape of the strain distributions across the splice ends of the specimen. Therefore, the strain distributions provide an indication to the behavior of the splices in a section where a number of bars are spliced.

3.2.3 Bar Strains along Splice. Distribution of steel strain along a splice is obtained from gages located at intervals along the splice length, as shown in Appendix 1. Figures 3.25 through 3.27 show strain distributions along the splice for typical specimens, for both edge and interior splices. As shown in Appendix 1, full instrumentation along the splice length was used for both bars in one of the outside edge splices in the cross section. Also, one or more of the interior splices was instrumented, with one bar of the lapped pair being gaged, in order to study the distribution of strain between the interior and exterior bars along the splice length.

Since the rate of variation of bar stress (or strain) along the splice length is proportional to the local bond stress along the bar, the rate of change of the strain along the lap length represents the bond stress developed along the splice length [3]. At low loading on the specimen, stress transfer for the lapped splice can occur in a relatively short length of lap near the ends of the splice. The strain is changing little at the interior third of the splice, indicating that very little stress is transferred over this portion of the splice. As loading is increased, the stress transfer requirements increase, and the rate of change of strain becomes nearly uniform over the entire splice length, indicating the development of higher bond stresses further along the splice. For specimens in which the steel yields before the splice fails, the strain distributions along the splice may not exhibit a nearly constant slope [3].

Study of the strain distributions along the exterior and interior splices can give insight into the splice behavior. At loads below the

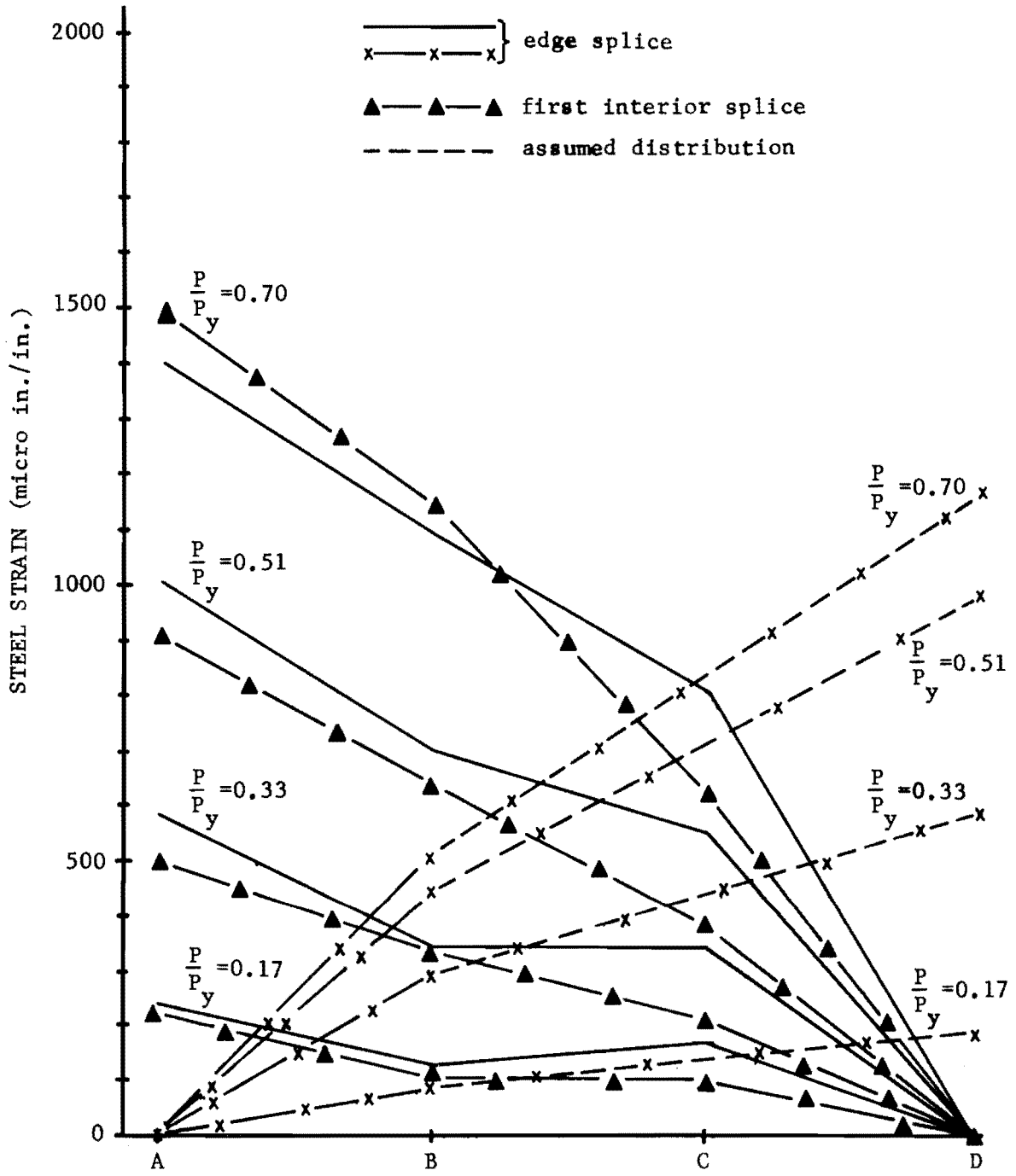

Fig. 3.25. Strain distributions along splice length for specimen 11-30-4/2/4-6/6

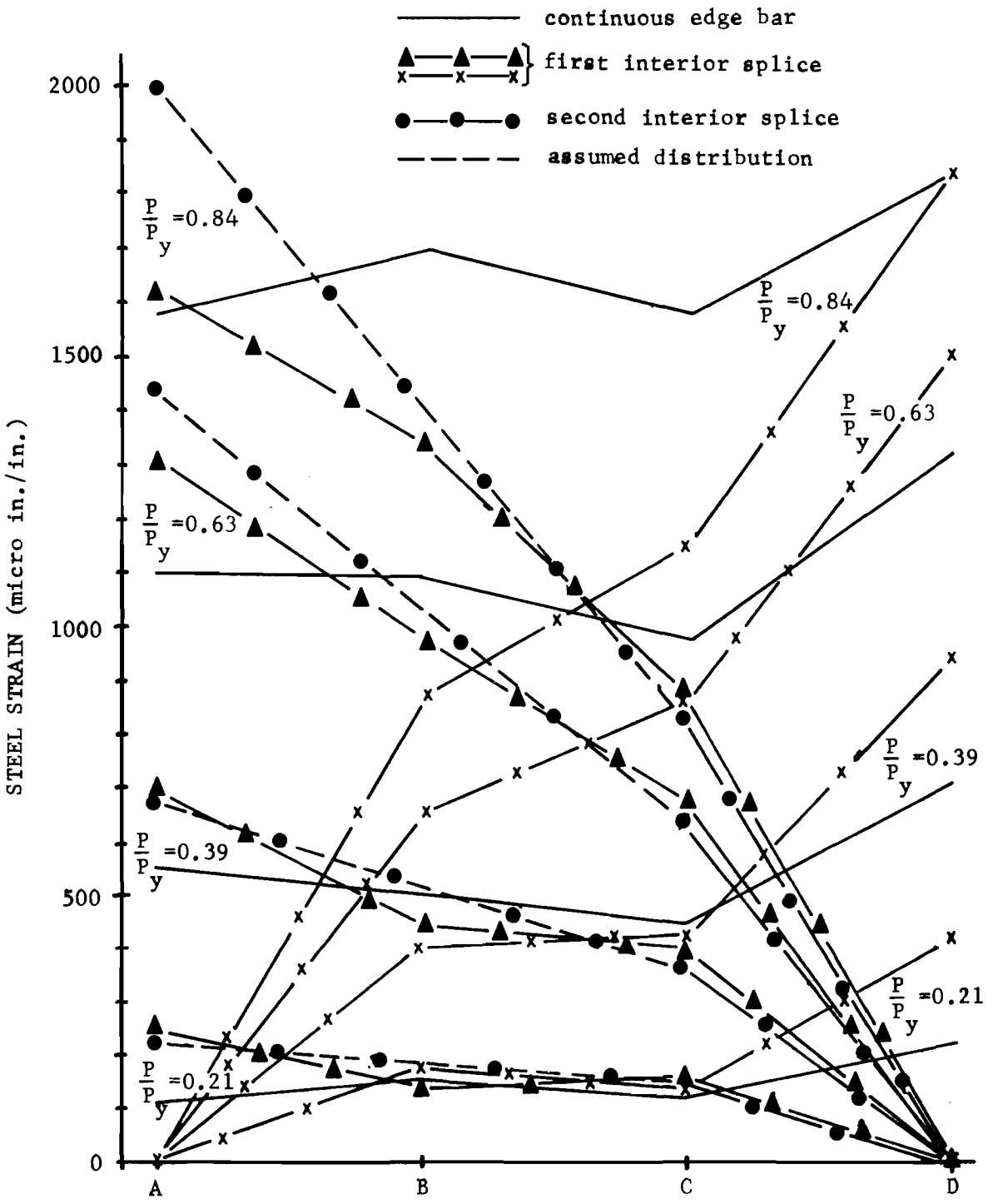

Fig. 3.26. Strain distributions along splice length for specimen 11-30-4/2/2.7-4/6

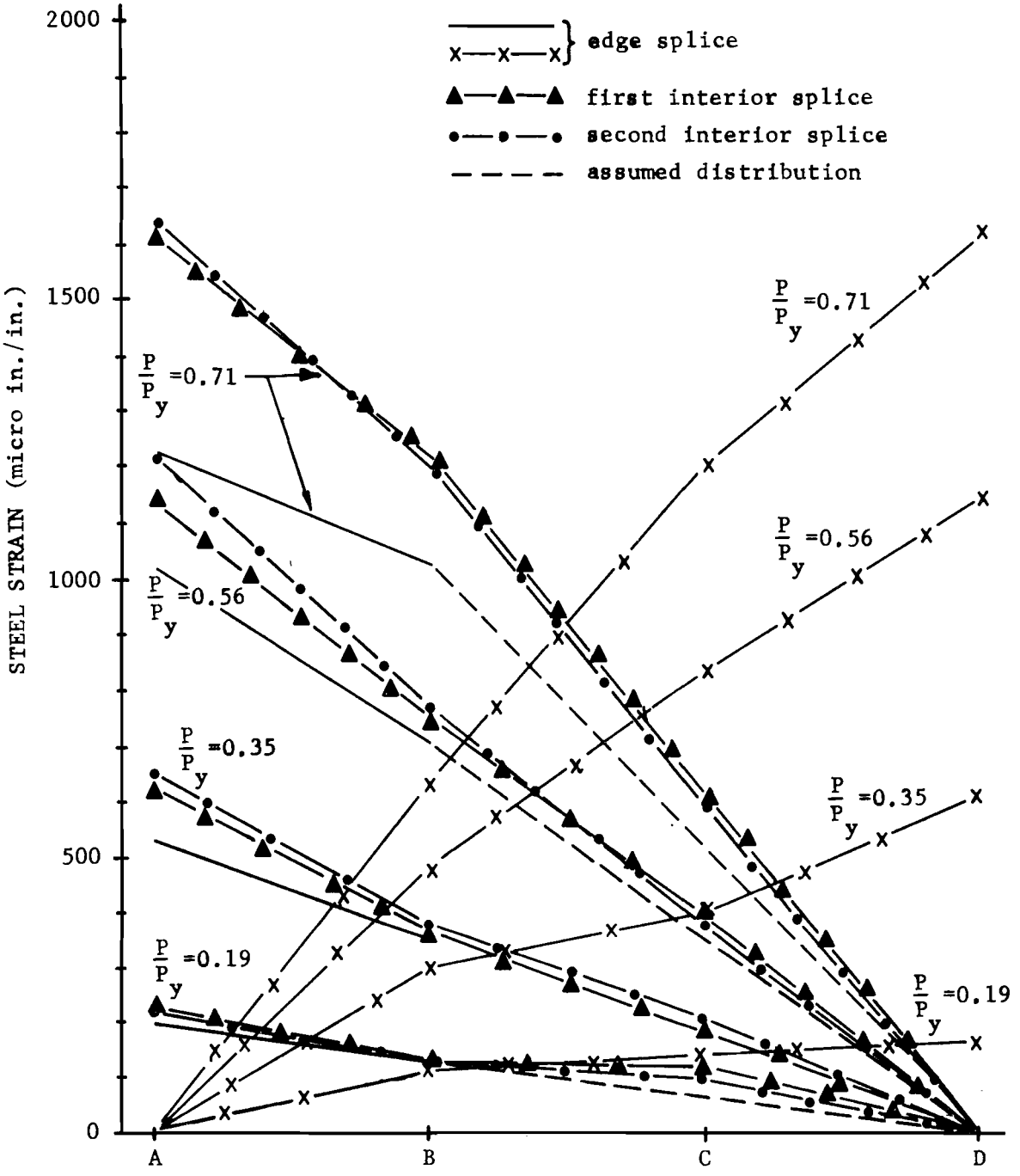

Fig. 3.27. Strain distributions along splice length for specimen 11-30-4/2/2-6/6-S5

failure load, the rate of change of the strain along the edge bars is generally equal to or greater than the rate of change along the interior splices (see Fig. 3.25). As failure of the specimen is approached, the rate of change of strain along the exterior bars tends to decrease, indicating a drop in bond stress along these bars. This is verified by the cracking patterns observed for specimens with all bars spliced in which the cracking prior to failure was concentrated around the edge splices. The strain distributions along interior splices exhibited a fairly constant slope near failure. It was noted that there was little cracking at interior splices prior to failure.

Figure 3.26 shows the strain distributions for a specimen with continuous edge bars. Strains are nearly uniform along the continuous edge bar that was instrumented. As shown in Appendix 1, the first interior splice next to this continuous edge bar was instrumented along both lapped bars. At failure, the rate of change of strain in one of these interior spliced bars (at the location of gage SS-A2) tends to decrease. This would seem to indicate that a high level of bond distress had been reached along the splice at this location. This corresponds to the cracking patterns of specimens with continuous edge bars, in which the first interior splice normally seems to be under the greatest splitting distress.

Strain distributions for a specimen with transverse reinforcement are shown in Fig. 3.27. The distributions show clearly the beneficial effects of transverse reinforcement in the splice region. The rate of change of strain along both exterior and interior splices seems to be nearly equal at low loads. Only near failure does the rate of change of strain for the outside edge splice exhibit a decrease, indicating a loss of capacity along this edge splice. The uniformity of stress transfer up to failure shows up in the cracking patterns of these specimens, in that splitting occurs over a large portion of the splice. The fact that the edge splice rate of change of strain decreases at failure relates to the face and side split failure mode for these specimens.

3.2.4 Strains Developed in Transverse Reinforcement. The tensile cracking strain of concrete is generally on the order of 100 μ-in./in. Considering a plane through the spliced bars, the concrete in this plane would be at cracking when the strain in the transverse reinforcement is on the order of 100 μ-in./in. Figures 3.28 through 3.31 show, for typical test specimens containing transverse reinforcement in the splice region, an average strain on the order of 400 μ-in./in. at failure of the specimens.

For Figs. 3.28 through 3.31, the strain in the transverse steel is plotted against the strain in the longitudinal bar at the end of the enclosed splice. Curves are plotted for stirrups located at various distances from the lead end of the splice (see Appendix 1).

Figure 3.28 seems to verify cracking of the concrete in the plane of the splice at a strain of about 100 μ-in./in. Upon reaching this strain, the rate of change of strain in the transverse steel seems to increase, indicating that the stirrups are picking up a larger amount of stress (or strain) per unit increase of stress (or strain) in the longitudinal reinforcement.

For a given strain in the longitudinal steel, the strain is lower in stirrups located further from the splice end. Stirrups near the splice end offer greater resistance to splitting of the tension surface than do the interior stirrups.

It should also be noted that the response of the stirrup closest to the splice end is fairly linear for interior splices (see Figs. 3.28 and 3.30). In general, the edge splices did not exhibit this linear relationship (see Figs. 3.29 and 3.31) which is further indication of the splitting distress associated with the behavior of the edge splices in a cross section.

Figures 3.28 and 3.30 show that when the failure of the specimen occurs the strains in transverse steel surrounding interior splices increased rapidly. Figures 3.29 and 3.31 show that for edge splices the strain in the transverse steel increases greatly prior to failure of the

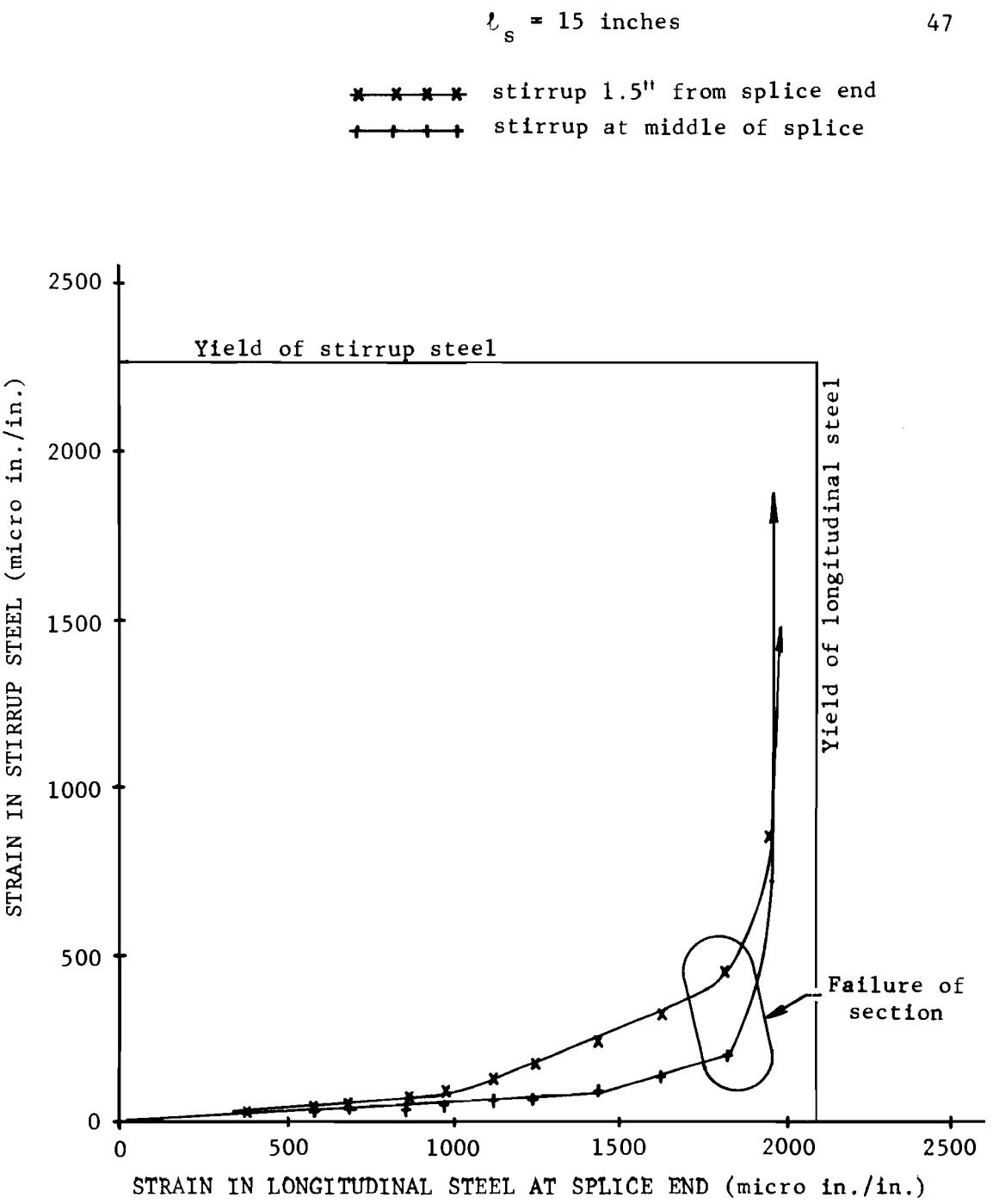

Fig. 3.28. Stirrup steel strain versus longitudinal steel strain for an interior splice (#3) for specimen 11-15-4/2/2-6/6-S5

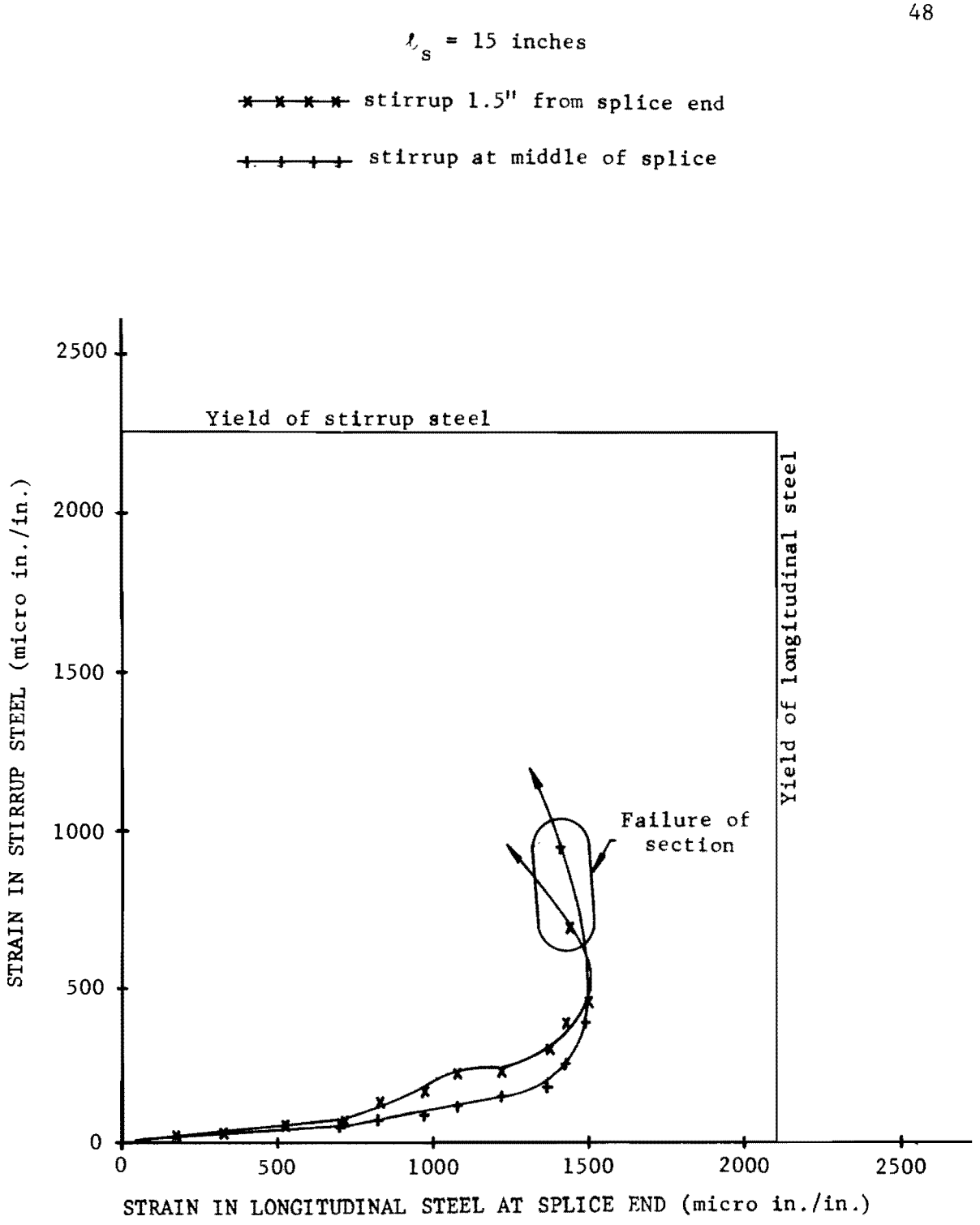

Fig. 3.29. Stirrup steel strain versus longitudinal steel strain for an edge splice (#1) for specimen 11-15-4/2/2-6/6-S5

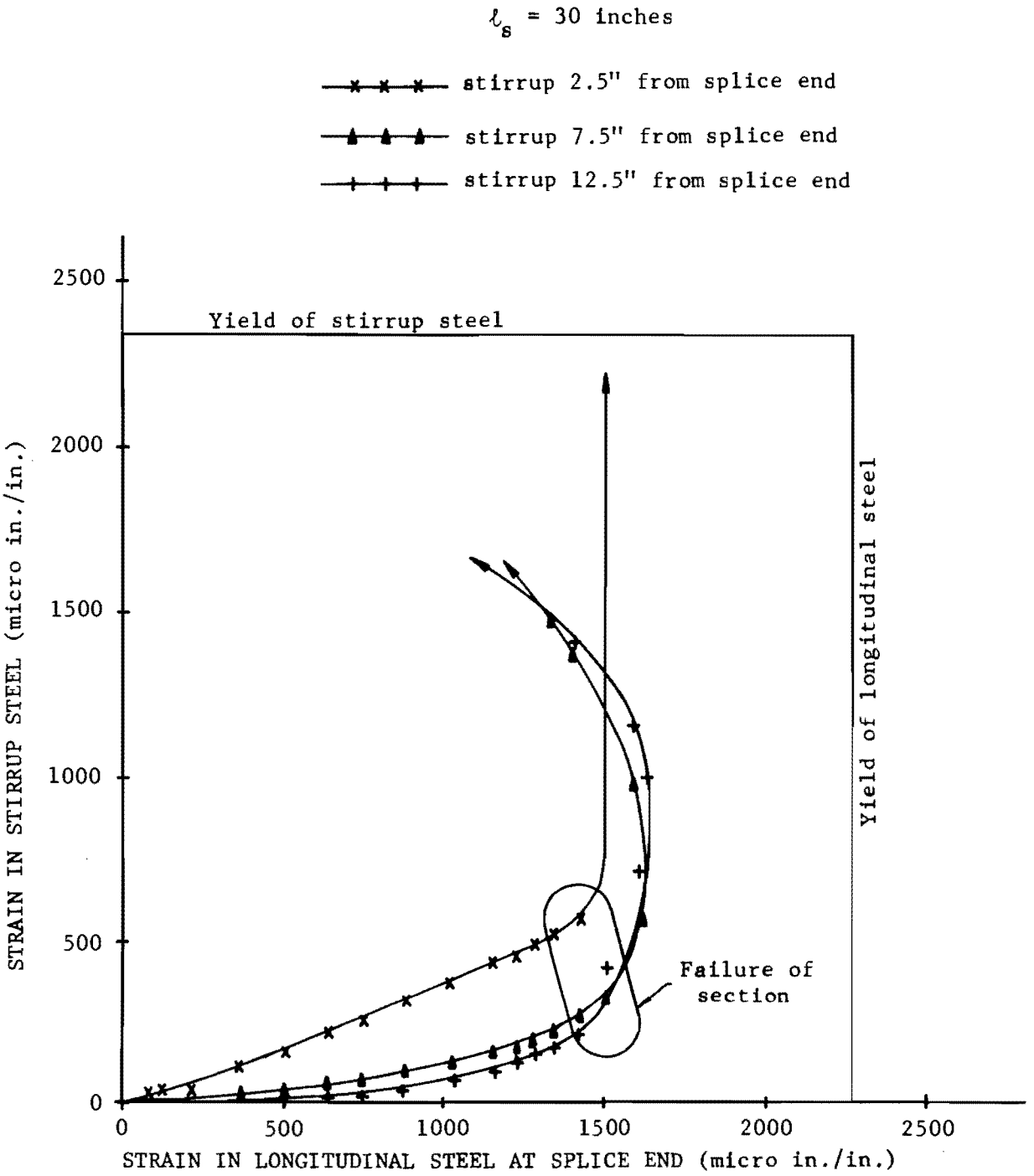

Fig. 3.30. Stirrup steel strain versus longitudinal steel strain for an interior splice (#2) for specimen 11-30-4/2/2-6/6-S5

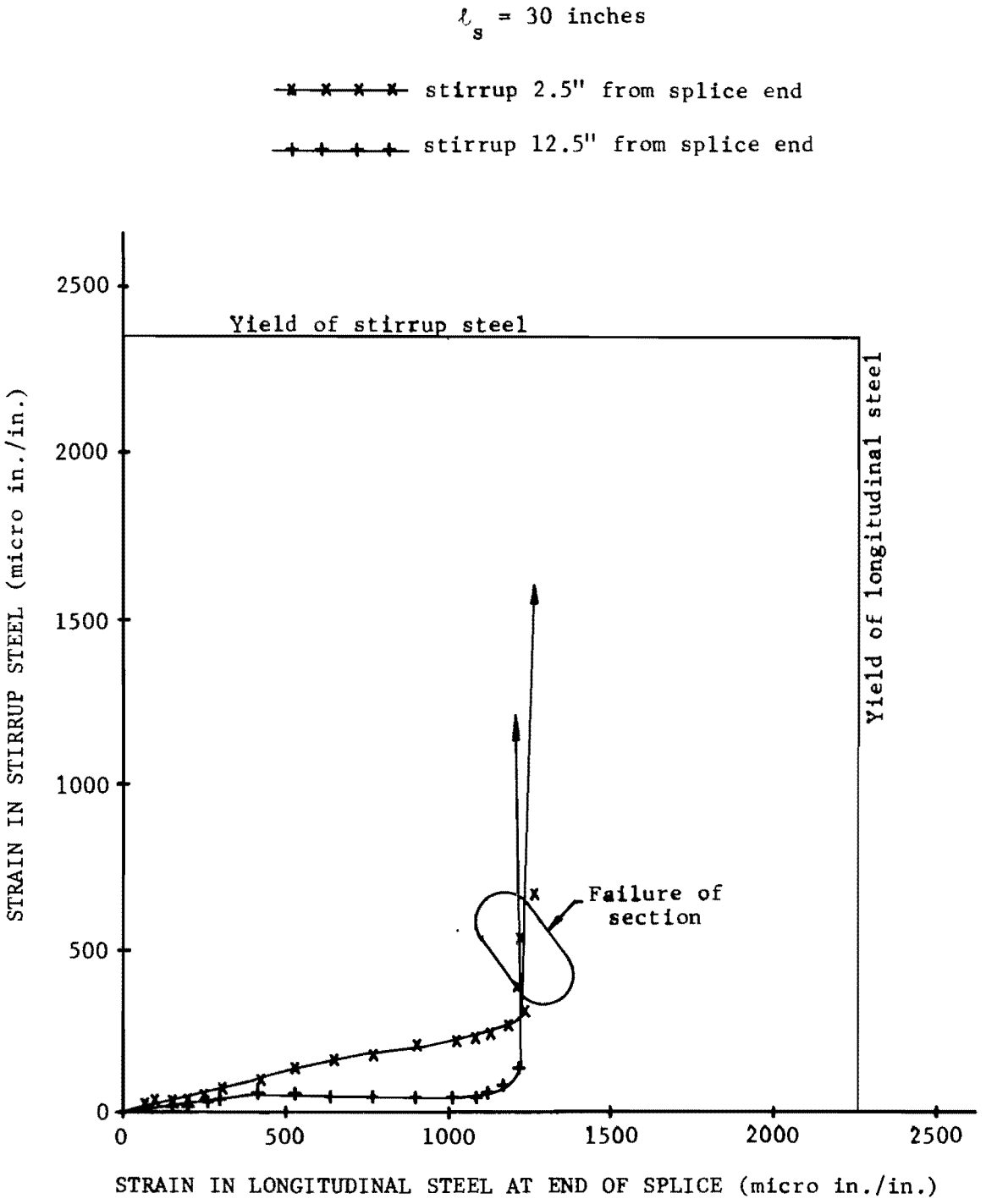

Fig. 3.31. Stirrup steel strain versus longitudinal steel strain for an edge splice (#1) for specimen 11-30-4/2/2-6/6-S5

specimen. This indicates edge splice failure precedes failure of the section which occurs when the capacity of the interior splices is exceeded.

3.2.5 Average Crack Widths. As stated previously, the widest flexural cracks in the constant moment region occurred at the ends of the splice. In certain cases, wide cracks at the splice ends could lead to a serviceability problem in reinforced concrete members containing lapped tension splices. For this reason, crack width measurements were made on the tension surface near the splice ends for each of the twenty-five specimens tested in this program.

Table 3.1 summarizes the average crack width across the splice end occurring with a working stress level in the longitudinal steel (approximately 36 ksi), for each of the twenty-five tests. One specimen failed before a stress level of 36 ksi could be reached in the steel; therefore, the maximum average crack width recorded (occurring at a stress level of 30 ksi) was tabulated for this one specimen.

Also shown in Table 3.1 is the maximum crack width measured on each specimen during testing. Because a sudden and brittle failure was expected in each of the tests, crack width measurements had to be abandoned as surface cracking became severe, and the maximum crack width recorded may not be that at failure in all cases.

By comparing the average crack widths at working stress (36 ksi) for the #8 and #11 splices tested (see Fig. 3.32), several general conclusions may be made. For a given clear cover over the bar, it appears that as the diameter of the bar is increased, the average crack width increases.

Previous studies [Ref. 5, Sec. 10.6 of Ref. 10] had indicated that the surface crack width varies almost linearly with the cover over the bar, and Fig. 3.32 seems to substantiate this relationship. Figure 3.32 also shows that crack widths in top cast specimens tended to be somewhat greater than in bottom cast specimens. It should be noted that the #11 bar top cast specimen failed before a working stress level could be reached in the steel.

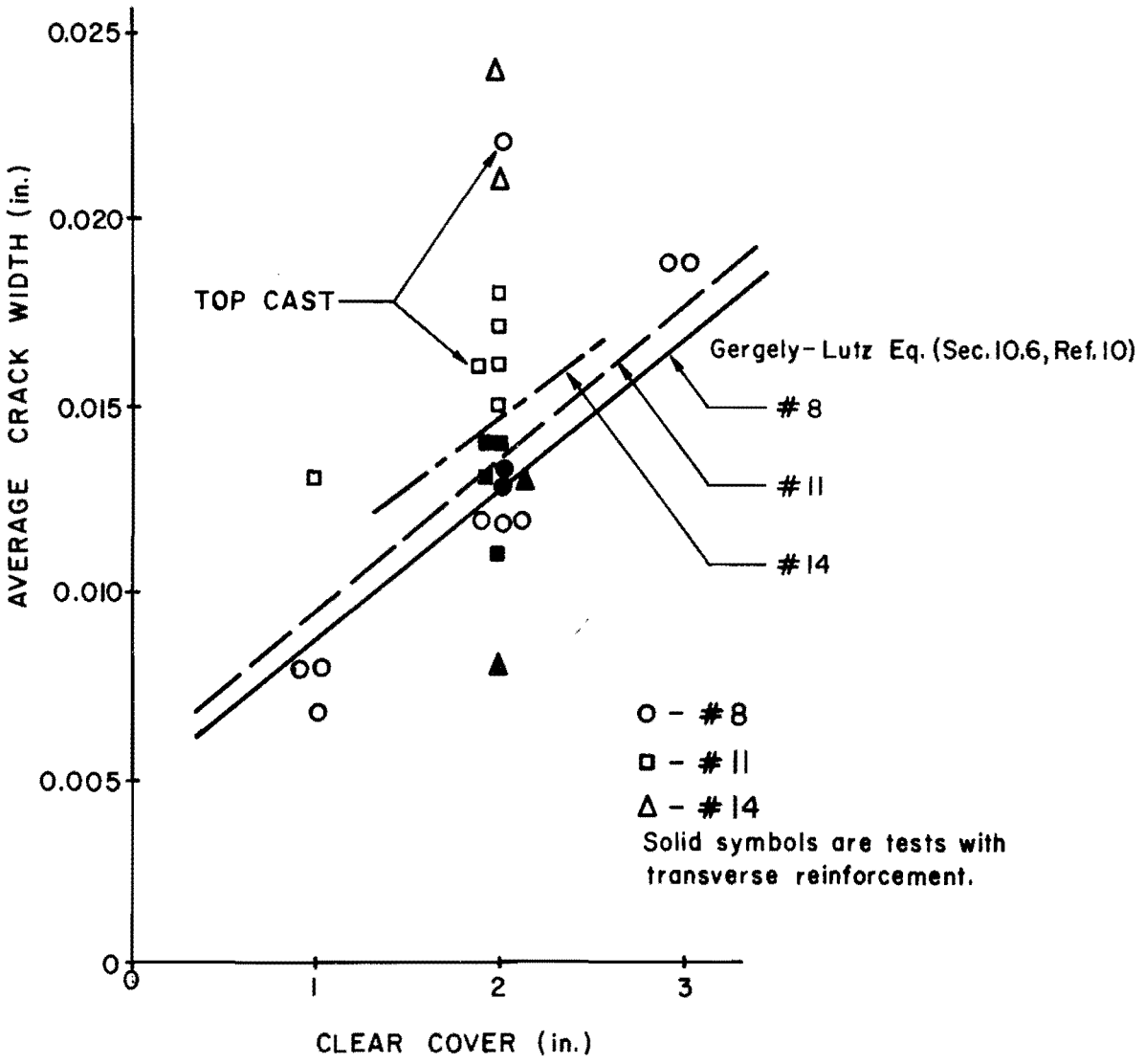

Fig. 3.32. Clear cover versus average crack width measured at splice ends

An empirical equation developed by Gergely and Lutz[10] forms the basis of crack control provisions in current specifications[3,9]. Crack widths for various cover thicknesses were calculated for the #8 and #11 specimens tested and the resulting curves are plotted in Fig. 3.32. As can be seen, the empirical equation predicts the crack width at working stress reasonably well in spite of the fact that splice lengths were fairly short and in some cases the splices may have been near failure at 36 ksi.

CHAPTER 4

EVALUATION OF TEST RESULTS

The performance of wide wall-type specimens containing lapped splices was documented with tests of twenty-five specimens in this program. The cracking patterns, reinforcing steel strain distributions, and failure modes of the specimens provide a means of establishing behavior of splices in wide sections. The purpose of this chapter is to evaluate the splice performance quantitatively.

In the first part of the chapter the importance of the various parameters introduced in the test program will be studied. In order to make comparisons, the level of average bond stress reached by similar specimens will be studied. The average bond stress can be calculated assuming that the tension force present in a bar at the end of a splice will be transferred to the concrete by an average longitudinal shearing stress acting on the surface of the bar along the splice length or

$$u(\pi d_b)\ell_s = \frac{\pi d_b^2}{4} f_s \qquad (1)$$

Rearranging,

$$u = \frac{f_s d_b}{4\ell_s} \qquad (2)$$

Because the strength of the concrete varied with specimens, average bond stresses will be normalized with regard to concrete tensile strength. It has been well documented that the splitting tensile strength of concrete varies as the square root of the compressive strength, provided the variation of compressive strength is not too large. In order to compare strengths of splice sections, it is possible to express results in a dimensionless ratio of the average bond stress divided by the square root of the compressive strength of the concrete.

The second purpose of this chapter is to evaluate the current ACI and AASHTO specifications for splices with regard to test results of the wide section splices. In addition a splice strength equation proposed in Reference [6], which includes parameters not considered in current ACI and AASHTO specifications, will be examined.

4.1 Evaluation of Specimen Variables

4.1.1 Splice Length and Bar Diameter. For a given size bar, it has been adequately demonstrated from test results [4] that the length of lap required to fully develop the yield stress of the steel in tension is dependent upon many parameters, including the concrete cover surrounding the splice, the amount of transverse reinforcement present in the splice, and the concrete strength. These studies have shown that the strength of a splice varies as a linear function of the splice length, provided that the bars do not reach yield stress.

This concept of a linear increase in strength with splice length seems to hold true for the tests on wide sections containing splices. Steel strain distributions plotted along the splice length for various specimens (Figs. 3.25 through 3.27) indicate that as the failure of a splice section is approached, the rate of change of steel strain along the length of the splice becomes essentially uniform. This rate of change of bar strain (or stress) is proportional to the local bond stress developed along the splice at failure. With an increase of splice length, it would seem reasonable that the same level of local bond stress could be achieved, resulting in a proportional increase in splice strength due to the additional splice length.

4.1.2 Ratio of Clear Bottom Cover to Clear Spacing of Splices. In an attempt to ensure that a splice failure would occur for each of the twenty-five specimens tested, a change in clear cover over the bars was compensated for by a corresponding change in the splice length. The result is that specimens cannot be compared directly in terms of ratios of clear cover to clear spacing. However, it seems possible to compare

specimens in terms of the dimensionless ratio $u/\sqrt{f'_c}$. Table 4.1 shows the tabulation of this parameter for some of the #8 and #11 bar tests.

These comparisons indicate that the strength of the splice is increased as the ratio of the clear cover to the clear spacing is increased. The clear spacing (4 in.) is constant in all the tests listed.

4.1.3 Edge Condition. Observation of the behavior of wide sections containing all bars spliced indicates the edge splices in the section may be the weakest splices and precipitate failure of the section. Four specimens were tested with edge cover equal to the clear spacing between splices. Four similar specimens had edge cover equal to half the clear spacing. Three of the eight specimens reached yield during testing. A comparison of three pairs of the specimens is shown in Table 4.2, expressed in terms of the ratio $u/\sqrt{f'_c}$. These results indicate that an increase in edge cover may increase the strength of the splice section slightly, up to 14 percent for the specimens tested. It should also be noted that increased edge cover did not normally alter the failure mode of the specimens.

Four specimens which contained continuous edge bars were tested, and were compared with four similar specimens which had spliced edge bars. Four of the eight specimens reached yield during testing. A comparison of three pairs of the tests is shown in Table 4.3, and indicates a change of strength from 0 to +13 percent associated with the use of continuous edge bars. In one pair of tests, a very slight decrease was noted, however, this can be attributed to very high concrete strength (f'_c = 4710 psi). The remaining four tests compared exhibit an increase in splice strength with continuous edge bars.

As noted earlier, the edge splices in a wide section containing all bars spliced seemed to be under the greatest splitting distress prior to failure of the splice section. However, failure of the section as a whole did not seem to occur until the capacity of the interior splices

TABLE 4.1. EFFECT OF INCREASE IN RATIO c/S' ON STRENGTH OF SPLICE SECTION FOR #8 AND #11 BAR TESTS

Specimen	f'_c psi	f_s ksi	c/S'	$\frac{u}{\sqrt{f'_c}}$
8-36-4/1/2-6/6	2525	59.3-Y	0.25	8.20
8-24-4/2/2-6/6	3100	53.5	0.50	10.00
8-18-4/3/2-6/6	4710	57.9	0.75	11.72
11-45-4/1/2-6/6	3520	44.0	0.25	5.86
11-30-4/2/2-6/6	2865	39.4	0.50	8.65

TABLE 4.2. EFFECT OF INCREASE IN EDGE COVER ON STRENGTH OF SPLICE SECTION FOR #8 AND #11 BAR TESTS

Specimen	f'_c psi	f_s ksi	$\frac{u}{\sqrt{f'_c}}$	Percent Increase
8-36-4/1/2-6/6	2525	59.3-Y		
8-36-4/1/4-6/6	2910	59.3-Y		
8-24-4/2/2-6/6	3105	53.5	10.00	
8-24-4/2/4-6/6	3760	59.3-Y	10.07	0.7
11-30-4/2/2-6/6	2865	39.4	8.65	
11-30-4/2/4-6/6	3350	44.1	8.95	3.5
14-60-4/2/2-5/5	2865	44.6	4.90	
14-60-4/2/4-5/5	3200	53.8	5.59	14.1

TABLE 4.3. EFFECT OF CONTINUOUS EDGE BARS ON THE STRENGTH OF SPLICE SECTION FOR #8 AND #11 BAR TESTS

Specimen	f'_c psi	f_s ksi	$\frac{u}{\sqrt{f'_c}}$	Percent Increase
8-18-4/3/2-6/6	4710	57.9	11.72	
8-18-4/3/2.5-4/6	2920	45.4	11.67	-0.4
8-36-4/1/2-6/6	2525	59.3-Y		
8-36-4/1/2.5-4/6	3440	59.3-Y		
8-24-4/2/2-6/6	3105	53.5	10.00	
8-24-4/2/2.5-4/6	3375	59.3-Y	10.63	6.3
11-30-4/2/2-6/6	2865	39.4	8.65	
11-30-4/2/2.7-4/6	4420	55.3	9.77	12.9

had been reached. Based on test results, increased edge cover or the use of continuous edge bars (or staggered splices) may provide up to about a 10 percent increase in total splice strength. For a typical wall splice, in which a large percentage of the splices would be interior splices, a modification of the edge splices probably would not affect the total splice strength as greatly as observed in the test program.

4.1.4 Transverse Reinforcement. It has been well-documented by other researchers that the addition of transverse reinforcement in the splice region leads to an overall improvement in splice performance [1,2]. The beneficial effects of transverse reinforcement were noted also in the present series of tests on wide spliced sections. In general splice strength was increased, and cracking reduced with the addition of transverse reinforcement.

Table 4.4 shows the effect of transverse reinforcement on the strength of the splice section of the specimens tested. It is noted the addition of transverse reinforcement in the splice region always results in a strength increase of the splice section for the specimens tested. The increase seems to range from about 10 to 90 percent, depending upon the amount of transverse reinforcement supplied. The specimens with #14 bars containing transverse reinforcement displayed a significant strength increase and were able to reach yield.

Comparisons of the #11 bar tests containing transverse reinforcement indicate the specimen containing spiral reinforcement had the strongest splices. This seems reasonable since the spiral would be most effective in resisting the radial stress in the concrete due to the stress transfer.

It should be noted again that an increase in splice strength was not the only beneficial result of transverse reinforcement in the splice section. Generally cracking was less severe (see Fig. 3.32). The failure of the specimens was less brittle than that of similar specimens not containing transverse reinforcement (see Fig. 3.16). These beneficial effects would tend to make the use of transverse reinforcement in the splice region a viable consideration in splice design.

4.1.5 Casting Position. Table 4.5 relates the decrease in splice strength associated with the top casting of main reinforcement. The strength decrease varies greatly for the two tests, with the maximum reduction about 16 percent. A reduction in strength due to top casting is a combination of several factors, all of which may not have been present for the specimens tested in the program. For vertically cast bars typical in retaining wall structures, the data obtained using bottom cast specimens are likely a better indication of performance than that from the top cast specimen.

4.2 Evaluation of Current ACI and AASHTO Specifications and Proposed Design Equation

4.2.1 Current Specifications. In all tests, the splice section was a region of high tensile stress in the bars ($f_s > 0.5f_y$) and more

TABLE 4.4. EFFECT OF TRANSVERSE REINFORCEMENT ON THE STRENGTH OF SPLICE SECTION FOR #8, #11 and #14 BAR TESTS

Specimen	f'_c psi	f_s ksi	$\frac{u}{\sqrt{f'_c}}$	Percent Increase
8-24-4/2/2-6/6	3105	53.5	10.00	
8-15-4/2/2-6/6-S5	3510	54.1	15.22	52.2
11-30-4/2/2-6/6	3865	39.4	8.65	
11-30-4/2/2-6/6-S5	3060	45.0	9.56	10.5
11-30-4/2/2-6/6	2865	39.4	8.65	
11-20-4/2/2-6/6-S5	3400	35.0	10.58	22.3
11-30-4/2/2-6/6	2865	39.4	8.65	
11-20-4/2/2-6/6-S2.9	3620	42.1	12.33	42.5
11-20-4/2/2-6/6	2865	39.4	8.65	
11-20-4/2/2-6/6-SP	3265	41.3	12.75	47.3
14-60-4/2/2-5/5	2865	44.6	5.88	
14-40-4/2/2-5/5-S3	3010	57.7-Y	11.13	89.3
14-60-4/2/2-5/5	2865	44.6	5.88	
14-40-4/2/2-5/5-S5.7	3500	57.7-Y	10.32	75.5

TABLE 4.5. EFFECT OF TOP CASTING OF REINFORCEMENT ON THE STRENGTH OF SPLICE SECTION FOR #8 AND #11 BAR TESTS

Specimen	f'_c psi	f_s ksi	$\frac{u}{\sqrt{f'_c}}$	Percent Decrease
8-24-4/2/2-6/6	3105	53.5	10.00	
8-24-4/2/2-6/6-TC	2640	47.7	9.67	3.3
11-30-4/2/2-6/6	2865	39.4	8.65	
11-30-4/2/2-6/6-TC	2910	33.4	7.28	15.8

than half the bars were spliced at a section. Under these conditions, the splices are classified as Class C splices following current ACI and AASHTO specifications for splices. For #11 bars and smaller, the required splice length is

$$\ell_s = (1.7) \frac{0.04\ A_b\ f_y}{\sqrt{f'_c}} \tag{3}$$

The corresponding equation for the #14 bars is

$$\ell_s = (1.7) \frac{0.085\ f_y}{\sqrt{f'_c}} \tag{4}$$

Rewriting the above equations to solve for a steel stress in terms of splice length yields the following equations:

$$f_s = \frac{\ell_s \sqrt{f'_c}}{(1.7)\ 0.04\ A_b} \qquad \text{\#11 bars and smaller} \tag{5}$$

$$f_s = \frac{\ell_s \sqrt{f'_c}}{(1.7)\ 0.085} \qquad \text{\#14 bars} \tag{6}$$

Adjustments for the above equations are included in the ACI and AASHTO specifications. For top cast bars, the above Eqs. (5) and (6) should be divided by 1.4. For reinforcement spaced at least 6 in. on center at least 3 in. from the side face of the member, the Eqs. (5) and (6)

should be multiplied by 1.25. Strength of splices enclosed within a spiral which is not less than 1/4 in. diameter and having a pitch not greater than 4 in. may be increased 33 percent.

Using the above Eqs. (5) and (6) and appropriate adjustments, stresses were calculated for each of the twenty-five specimens. Values of calculated steel stress using current recommendations are given in Table 4.6, Column I. A ratio of the measured average steel stresses at failure to the calculated stresses for each of the specimens is shown in Column II.

Examination of Column II reveals the current ACI and AASHTO specifications for splices always underestimate the strength of the wide splice sections tested in the program. This apparent conservatism is due to the fact that current design equations do not reflect all of the parameters which have been shown to be critical to splice strength. The test results indicate that the stress level at failure of the splice section may be as much as four times that predicted by current equations. Also, for the two top cast specimens the strength reduction exhibited was considerably less than would be indicated by current specifications which call for a 40 percent increase in splice length for top cast bars (see Table 4.5). As a result, a modification of design procedures may result in considerable economy without sacrificing safety.

4.2.2. Proposed Splice Strength Equation. Because the current ACI and AASHTO splice design equations greatly underestimate splice strength, the need for a reevaluation of splice design is apparent. Such a study was undertaken by Orangun, Jirsa, and Breen [6]. Test results on lap spliced beams and development length tests were used to develop a relationship between average bond stress and minimum cover, bar diameter, and splice length. The proposed equation was also modified to reflect the influence of transverse reinforcement in the splice region.

The basic proposed equation is:

$$u/\sqrt{f'_c} = 1.2 + 3\frac{C}{d_b} + 50\frac{d_b}{\ell_s} + \frac{A_{tr} f_{yt}}{500 s d_b} \qquad (7)$$

TABLE 4.6. COMPARISONS OF CURRENT AND PROPOSED EQUATIONS WITH MEASURED TEST STRESSES

Specimen	Test Results				Current Provisions		Proposed Equation		
	Failure Mode*	f'_c psi	f_s (Average)	f_s (Edge)	f_s (Current) I	Average Current II	f_s (Proposed) III	Average Proposed IV	Edge Proposed V
6-12-4/2/2-6/6	F-S	3730	55.9	46.4	24.5	2.28	48.2	1.16	0.96
8-18-4/3/2-6/6	F	4710	57.9	51.2	23.0	2.52	49.3	1.17	1.04
8-18-4/3/2.5-6/6	C-F	2920	45.4	45.3	18.1	2.51	38.8	1.17	1.17
8-36-4/1/2-6/6	F-S-Y	2520	59.3-Y	46.7	33.7	1.76	40.4	1.47	1.16
8-36-4/1/2.5-4/6	Flex	3440	59.3-Y	59.3-Y	39.3	1.51	47.2	1.26	1.26
8-36-4/1/4-6/6	C-F-Y	2910	59.3-Y	59.3-Y	36.2	1.64	43.4	1.37	1.37
8-24-4/2/2-6/6	F-S	3105	53.5	51.3	24.9	2.15	49.7	1.08	1.03
8-24-4/2/2.5-4/6	C-F-Y	3375	59.3-Y	59.3-Y	26.0	2.28	51.8	1.14	1.14
8-24-4/2/4-6/6	F-S-Y	3760	59.3-Y	59.3-Y	27.4	2.16	54.6	1.09	1.09
8-15-4/2/2-6/6-S5	F-S	3510	54.1	41.3	16.5	3.28	47.6	1.14	0.87
8-24-4/2/2-6/6-TC	F-S	2640	47.7	27.8	16.4	2.91	35.2	1.36	0.79
11-45-4/1/2-6/6	F-S	3520	44.4	37.9	25.2	1.76	37.1	1.20	1.02
11-30-4/2/2-6/6	F-S	2865	39.4	33.6	15.1	2.61	35.6	1.11	0.94
11-30-4/2/4-6/6	F-S	3350	44.1	40.5	16.4	2.69	38.6	1.15	1.05
11-30-4/2/2.7-4/6	C-F	4420	55.3	55.3	18.8	2.94	44.2	1.25	1.25
11-25-6/2/3-5/5	F-S	3920	40.0	28.7	18.4	2.17	36.8	1.09	0.78
11-20-4/2/2-6/6-S5	F-S	3400	35.0	26.7	11.1	3.15	36.7	0.95	0.73
11-20-4/2/2-6/6-S2.9	F-S	3620	42.1	37.6	11.3	3.73	41.0	1.03	0.92
11-30-4/2/2-6/6-S5	F-S	3060	45.0	35.6	15.7	2.87	46.8	0.96	0.76
11-20-4/2/2-6/6-SP	F-S	3265	41.3	26.1	14.4	2.87	38.9	1.06	0.67
11-30-4/2/2-6/6-TC	F-S	2910	33.4	28.2	10.9	3.06	27.5	1.21	1.03
14-60-4/2/2-5/5	F-S	2865	44.6	40.9	22.2	2.01	46.7	0.96	0.88
14-60-4/2/4-5/5	F-S	3200	53.8	49.2	23.5	2.29	49.3	1.09	1.00
14-40-4/2/2-5/5-S3	Flex	3010	57.7-Y	57.7-Y	15.2	3.80	50.1	1.15	1.15
14-40-4/2/2-5/5-S5.7	F-S-Y	3500	57.7-Y	57.7-Y	16.4	3.38	46.8	1.18	1.04
				Average Ratio		2.57		1.15	1.00
				σ		0.63		0.12	0.10

*F-S Face and Side Split
F Face Split
C-F Confined Face Split
Flex Flexural Failure
Y Yielding of Longitudinal Steel

Solving for steel stress, the following equation is obtained:

$$f_s = \frac{4\ell_s}{d_b}\left(1.2 + 3\frac{C}{d_b} + 50\frac{d_b}{\ell_s} + \frac{A_{tr}f_{yt}}{500sd_b}\right)\sqrt{f'_c} \qquad (8)$$

The following limitations are suggested. The value of $A_{tr}f_{yt}/500sd_b$ should not be taken as being greater than 3. The value of C/d_b used should not exceed 2.5. For top cast reinforcement, the above equations should be divided by 1.30.

Using the above Eq. (8) and applicable factors, steel stresses were calculated for each of the twenty-five tested, and are shown in Column III of Table 4.6. Column IV gives a ratio of the measured average steel stress level at failure to the stress calculated using the proposed equation. In Column V, a similar ratio is made using the lowest level of stress measured in an edge splice for each of the tests.

Examination of Column IV indicates excellent agreement between the steel stress calculated using the proposed splice strength equation and the test results of wide sections. The average ratio of measured to calculated stress (1.15) is much lower than that based on current Code recommendations (2.57). Only three of the tests exhibited measured stress levels less than the calculated stress levels, with the lowest ratio of measured to calculated being 0.95.

The conservatism exhibited by the proposed equation when applied to wide splice sections can be explained by the data on which the equation is derived. Virtually all available test results are for specimens with one or two spliced bars, in which the splices in the sections behaved essentially as edge splices. Thus, the proposed equation is based primarily on data obtained from tests of edge splices. As noted by the test results on wall type specimens, the edge splices in a section are normally the first to show splitting distress, with the failure of the section as a whole occurring when the interior splices failed. This would seem to indicate an interior splice may be somewhat stronger than an edge splice, which would mean the proposed equation underestimates the strength of wide splice sections.

Using the wall-test data, a link between the mode of failure and predicted stress can be seen. For specimens which failed in either the face or side split or the face split mode of failure, and did not contain transverse reinforcement in the splice region, the proposed splice strength equation seems to more accurately predict the stress levels of the edge splices in a wide section rather than the average stress levels developed by the specimens (Average Ratio = 1.00, σ = 0.10). This could be expected, since the proposed equation is based essentially on test results of edge splices as explained above. Also the results in Column IV for specimens which failed in a confined face split mode of failure indicate the proposed equation may be most conservative for these specimens. This can be understood since all of the splices in such a section are behaving essentially as interior splices.

It becomes difficult to predict the failure mode of any general cross section containing lap splices, and thus a rational design equation based on parameters which have been shown to be critical to splice strength seems to be a reasonable approach. Because the proposed equation is based on tests of edge splices, the results obtained from the use of the proposed equation on wide wall-type cross sections should be conservative. Although interior splices in such a section may be slightly stronger than the edge splices, an adjustment in the predicted strength of the section to account for this is not deemed necessary.

CHAPTER 5

SUMMARY AND CONCLUSIONS

5.1 Summary

Twenty-five tests were conducted to study the behavior of reinforcing bar lap splices in a wall. Special attention was given to the degree that edge splices affect the strength of the splice section as a whole. Six lap splices were used for the splice section of the #6, #8, and #11 bar specimen tests, with five lap splices used in the #14 bar tests. The width of the sections varied from 33 to 45 in. Specimens were designed so that a splice failure occurred before the steel reached yield. A two point loading system was used to produce a constant moment along the splice section. Cracking patterns, steel strain distributions, and failure modes were observed and categorized.

The following failure patterns were observed with the wide specimens tested:

(a) Face and Side Split. Failure of the splice section occurred with the corners of the tension surface around the edge splices breaking free and the cover over the interior splices lifting up and splitting. The edge splices in such a section appeared to be under the greatest splitting distress. Correlation was exhibited with the steel strain distributions across the end of the splices, which showed the steel strain in the interior splices as failure of the section was approached. This mode of failure seemed to occur when the edge cover was about equal to the clear cover on the specimen.

(b) Confined Face Split. For specimens having either an edge cover greater than twice the clear cover or containing continuous edge bars, the failure pattern could be described as a confined face split. Failure of the section occurred with lifting of the cover over the interior splices between the edge bars without involving a corner element of the splice section. No splitting cracks were observed on the sides of the

specimens failing in this manner. The steel strain distributions across the splice ends indicated the edge splices in such a section performed as well as the interior splices.

(c) Face Split. This failure mode occurred for a specimen which had edge cover less than the clear cover. The failure surface was a horizontal plane passing through the splices, with the cover lifting over all of the splices. Splitting cracks did not appear on the tension surface of the specimen prior to failure. Failure of the section was initiated by splitting cracks forming on the side surfaces of the sections. Steel strain distributions across the end of the splice indicated that the failure was initiated at the edge and progressed inward. Failure of the section occurred soon after the formation of the side splitting cracks.

For the specimens tested in this program, the V-type failure noted in other splice tests was not observed. This is probably due to the fact that the spacing of the splices relative to the clear cover thickness was too small for this failure to occur.

The factors affecting the strength of lapped splices in a wall-type section and their influence are as follows:

(a) Lap Length. For a given bar size, an increase in the length of the lap will result in an increase in splice strength, provided the bars do not yield.

(b) Ratio of Clear Cover to Clear Spacing. For a given clear spacing between the splices, the strength of a splice increases with increased clear cover.

(c) Edge Condition. The edge splices in a section normally proved to be the weakest splices, provided the clear cover was not small enough for a confined face split failure to occur.

(d) Transverse Reinforcement. The inclusion of transverse reinforcement in the splice section led to an overall improvement in the splice performance. Splice strength was increased and cracking reduced. Spiral reinforcement appeared to most effectively confine the splitting distress

associated with the differential strains between the spliced bars, although the use of spirals would probably be limited in the field.

(e) Casting Position. A decrease in splice strength was noted with the top casting of the main reinforcement. It is felt that the bottom cast specimens most closely match the conditions in a vertically cast wall splice region.

(f) Concrete Strength. As the tensile strength of the concrete is increased, the strength of the splice is increased. For design purposes the tensile strength of the concrete can be considered to vary as the square root of the compressive strength.

5.2 Conclusions

Based on the test results obtained in this study, the following conclusions can be made:

(1) Increased edge cover or the use of continuous edge bars in a wide section may provide up to about a 10 percent increase in total splice section strength. In general, the strength of a section seems to be governed by the capacity of the interior bars, such that a modification of edge conditions does not appear warranted for design

(2) Prevailing ACI and AASHTO Code provisions for length of splices were overly safe when applied to the wide specimens tested in this program. The strength of the specimens as tested ranged from between 1.5 to 4 times the strength as predicted by the current provisions. The large difference between the predicted and the measured strength can be attributed to the omission from current provisions of many parameters shown to be critical to splice strength. Because current splice design provisions appear to greatly underestimate splice strength, a reevaluation of splice design was undertaken in an accompanying phase of this project [6]. The proposed equation presented in this accompanying report is based primarily on data obtained from tests of edge splices. Although test results from this study on wide sections containing multiple lap splices indicate that edge splices may be somewhat weaker than interior

splices, a modification of the proposed equation to predict wide section splice strength was not deemed necessary. The results of the tests in this program compared very favorably with the strengths predicted using the empirical equation developed in the accompanying study.

REFERENCES

1. Briceno, Eduardo A., "Development Length for Spliced Bars in Concrete Beams and Walls," Unpublished Ph.D. dissertation, The University of Texas at Austin, May 1969.

2. Krishnaswamy, C. N., "Tensile Lap Splices in Reinforced Concrete," Unpublished Ph.D. dissertation, The University of Texas at Austin, December 1970.

3. Building Code Requirements for Reinforced Concrete (ACI 318-71), American Concrete Institute, Detroit, 1971.

4. Ferguson, Phil M., "A New Look at Bond and Splicing in Reinforced Concrete," class notes from CE 383L, The University of Texas at Austin, Fall 1973.

5. Ferguson, Phil M., Reinforced Concrete Fundamentals, Third Edition, John Wiley and Sons, Inc., New York, June 1972.

6. Orangun, C. O., Jirsa, J. O., and Breen, J. E., "The Strength of Anchored Bars: A Reevaluation of Test Data on Development Length and Splices," Research Report No. 154-3F, Center for Highway Research, The University of Texas at Austin, January 1975.

7. Ferguson, P. M., and Briceno, E. A., "Tensile Lap Splices - Part 1: Retaining Wall Type, Varying Moment Zone," Research Report No. 113-2, Center for Highway Research, The University of Texas at Austin, July 1969.

8. Ferguson, P. M., and Krishnaswamy, C. N., "Tensile Lap Splices - Part 2: Design Recommendations for Retaining Wall Splices and Large Bar Splices," Research Report No. 113-3, Center for Highway Research, The University of Texas at Austin, April 1971.

9. AASHTO Subcommittee on Bridges and Structures, Interim Specifications, Bridges, 1974, American Association of State Highway and Transportation Officials, Washington, D.C., 1974.

10. Commentary on Building Code Requirements for Reinforced Concrete (ACI 318-71), American Concrete Institute, Detroit, 1971.

A P P E N D I X 1

LOCATION OF STRAIN GAGES

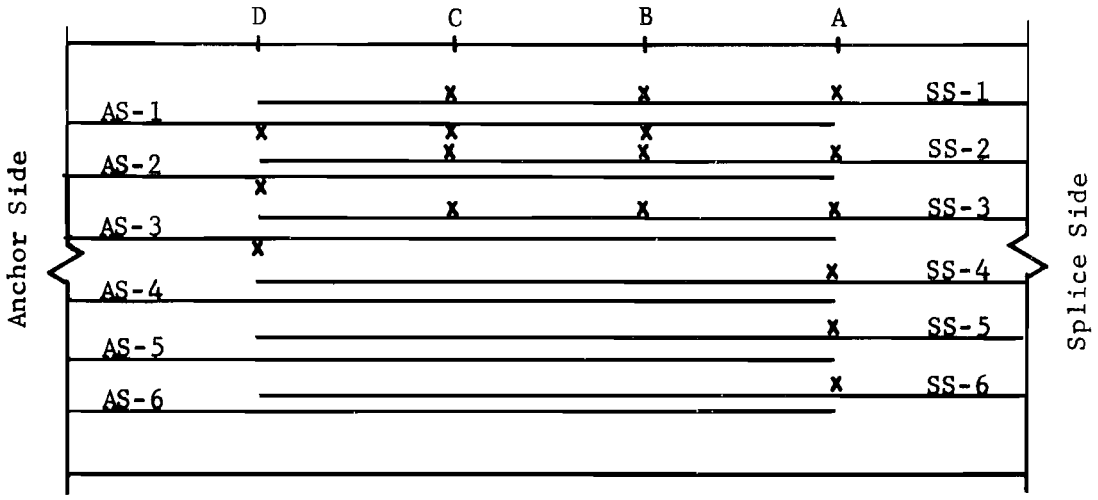

#6, #8, and #11 bar specimens with all bars spliced (as tested)

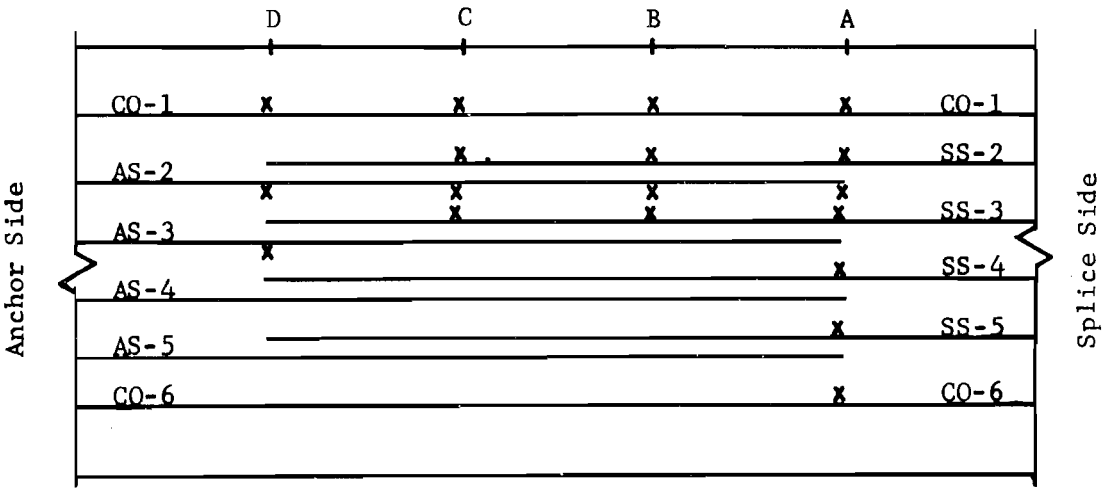

#8 and #11 bar specimens with continuous edge bars (as tested)

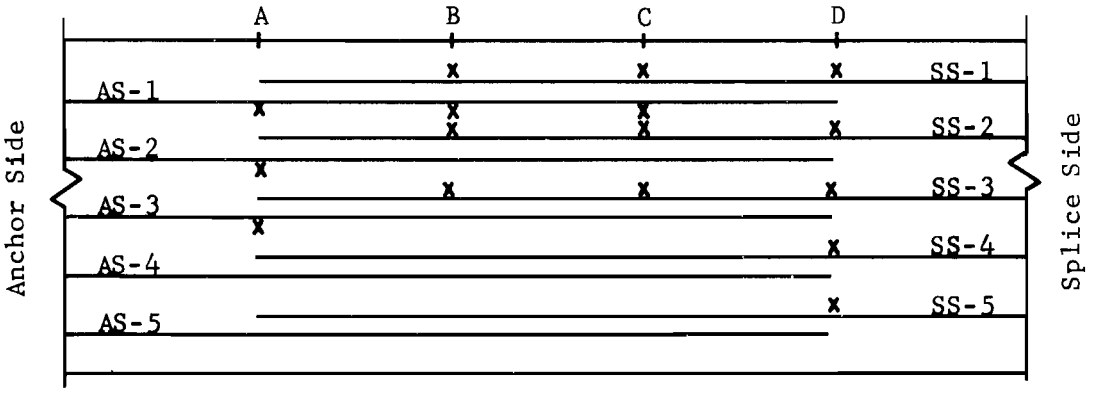

#14 bar specimens (as tested)

Detail of gage location on stirrups

A P P E N D I X 2

EQUIVALENT DEAD LOADS ON SPECIMENS

Specimen	Dead Moment at Splice Ends (in.-kips)	P_d (kips)
6-12-4/2/2-6/6	201.1	2.58
8-18-4/3/2-6/6	198.2	2.64
8-18-4/3/2.5-4/6	198.2	2.64
8-36-4/1/2-6/6	157.1	2.38
8-36-4/1/2.5-4/6	157.1	2.38
8-36-4/1/4-6/6	167.6	2.54
8-24-4/2/2-6/6	184.0	2.56
8-24-4/2/2.5-4/6	184.0	2.56
8-24-4/2/4-6/6	196.9	2.74
8-15-4/2/2-6/6-S5	205.3	2.68
8-24-4/2/2-6/6-TC	210.6	2.93
11-45-4/1/2-6/6	148.5	2.42
11-30-4/2/2-6/6	184.5	2.68
11-30-4/2/4-6/6	196.0	2.84
11-30-4/2/2.7-4/6	184.5	2.68
11-25-6/2/3-5/5	207.1	2.90
11-20-4/2/2-6/6-S5	210.0	2.84
11-20-4/2/2-6/6-S2.9	210.0	2.84
11-30-4/2/2-6/6-S5	184.6	2.68
11-20-4/2/2-6/6-SP	210.0	2.84
11-30-4/2/2-6/6-TC	211.8	3.07
14-60-4/2/2-5/5	236.4	3.03
14-60-4/2/4-5/5	253.6	3.25
14-40-4/2/2-5/5-S3	298.6	3.39
14-40-4/2/2-5/5-S5.7	298.6	3.39